Line-of-Sight $2 \times n_r$ MIMO With Random Antenna Orientations

Lakshmi Natarajan, Yi Hong, *Senior Member, IEEE*, and Emanuele Viterbo, *Fellow, IEEE*

***Abstract*—Line-of-sight (LoS) multiple-input multiple-output (MIMO) gives full spatial-multiplexing gain when the antenna array geometry and orientation are designed based on the interterminal distance. These known design methodologies that hold for antenna arrays with fixed orientation do not provide full MIMO gains for arbitrary array orientations. In this paper, we study LoS MIMO channels with random array orientations when the number of transmit antennas used for signaling is 2. We study the impact of common array geometries on error probability, and identify the code design parameter that describes the high signal-to-noise ratio (SNR) error performance of an arbitrary coding scheme. For planar receive arrays, the error rate is shown to decay only as fast as that of a rank 1 channel, and no better than SNR^{-3} for a class of coding schemes that includes spatial multiplexing. We then show that for the tetrahedral receive array, which uses the smallest number of antennas among nonplanar arrays, the error rate decays faster than that of rank 1 channels and is exponential in SNR for every coding scheme. Finally, we design a LoS MIMO system that guarantees a good error performance for all transmit/receive array orientations and over a range of interterminal distances.**

***Index Terms*—Antenna array, array geometry, coding scheme, line-of-sight, multiple-input multiple-output, probability of error.**

I. Introduction

The large swathes of raw spectrum available in the millimeter-wave frequency range are expected to provide an attractive solution to the high data-rate demands of the future 5G cellular networks [1]. The small carrier wavelength of millimeter-wave frequencies allows for reduced spacing between the antenna elements when multiple antennas are used at the transmitter and receiver. This implies that multiple-input multiple-output (MIMO) spatial multiplexing gains can be obtained even in the presence of a strong line-of-sight (LoS) component when operating in such high frequencies [2].

In LoS environment, the MIMO channel matrix $\mathbf{H}$ is a deterministic function of the positions of the transmitter and receiver and the geometry of the antenna arrays used at either terminals. If the positions of the communicating terminals are fixed and known *a priori*, the geometry of the antenna arrays can be designed to optimize the performance of the communication system. The LoS MIMO channel quality, in terms of capacity, multiplexing gain, coverage, and channel eigenvalues, has been studied in [2]–[9] as a function of the interterminal distance and the interantenna spacing of transmit and receive arrays, when the antennas are to be arranged in a rectangular, circular, or a linear array. However, these design techniques assume that the position and the orientation of the antenna arrays are fixed, and the resulting criteria may be difficult to be satisfied if either of the communicating terminals is mobile or if the positions of the wireless terminals are not known *a priori*. Systems designed according to these known criteria degrade gracefully with variations in the geometric parameters, and may be adequate in certain scenarios in which the changes in the orientation are limited, such as in a sectored communication cell where the variation of the base station orientation with respect to the direction of propagation is limited. However, these designs, which utilize two-dimensional (2-D) antenna arrays, do not provide MIMO spatial multiplexing gains for arbitrary array orientations.

In [10], the mutual information rates of a predominantly LoS channel with arbitrary antenna array orientations were studied using simulations and direct measurements in an indoor environment. The results show that the three-dimensional (3-D) antenna arrays obtained by placing the antennas on the faces of a tetrahedron or a octahedron provide mutual information rates that are largely invariant to the rotation of antenna arrays under indoor LoS conditions. Previous studies of 3-D antenna arrays for wireless communications have mainly studied the capacity of the resulting MIMO system in a rich scattering environment. In [11], a compact MIMO antenna was proposed that consists of 12 dipole antennas placed along the edges of a cube. A 24-port and a 36-port antenna were designed in [12] by placing antennas along the edges and faces of a cube. In [13] and [14], 6-port and 16-port antennas were designed on a cube, respectively, and the performance of the MIMO system in terms of capacity and channel eigenvalues in a richly scattering environment was studied. The objective of [11]–[14] has been to design a compact array by densely packing the antenna elements while exploiting the degrees of freedom available in an environment that provides abundant multipath components.

To the best of our knowledge, there has been no prior theoretical study of LoS MIMO channels where the transmit or receive antenna array orientations are arbitrary, as may be

Manuscript received January 28, 2016; revised August 28, 2016 and October 23, 2016; accepted November 7, 2016. Date of publication November 10, 2016; date of current version June 16, 2017. This work was supported by Australian Research Council Discovery Project under Grant ARC DP160100528. The review of this paper was coordinated by Prof. H.-F. Lu.

L. Natarajan is with the Department of Electrical Engineering, Indian Institute of Technology Hyderabad, Sangareddy 502285, India (e-mail: lakshminatarajan@iith.ac.in)

Y. Hong and E. Viterbo are with the Department of Electrical and Computer Systems Engineering, Monash University, Melbourne, VIC. 3800, Australia (e-mail: yi.hong@monash.edu; emanuele.viterbo@monash.edu).

Color versions of one or more of the figures in this paper are available online at http://ieeexplore.ieee.org.

Digital Object Identifier 10.1109/TVT.2016.2627537

experienced in wireless mobile communications. Furthermore, all previous works have focused on optimizing the mutual information rates of the MIMO channel. To achieve the information theoretic limits, we need code design criteria based on an error performance analysis of the communication channel. In this paper, we consider LoS MIMO channels where the number of transmit antennas used for signaling is 2 and both the transmit and receive arrays have random orientations. We study the impact of the geometry of the antenna arrays on the system error performance and design a LoS MIMO system that guarantees a minimum channel quality and good error performance for arbitrary transmit and receive orientations over a range of interterminal distances.

We model the 2-transmit antenna n_r-receive antenna LoS MIMO channel $\mathbf{H}$ using the upper triangular matrix $\mathbf{R}$ obtained from its QR-decomposition (see Section II). This allows us to derive bounds on pairwise error probability and identify the code parameter that determines the high signal-to-noise ratio (SNR) error performance of arbitrary coding schemes in LoS MIMO channels.

We show that for any planar, i.e., 2-D, arrangement of receive antennas (such as linear, circular, and rectangular arrays), the rate of decay of error probability is similar to that of a rank 1 LoS MIMO channel whenever the receiver undergoes random rotations. Furthermore, for some coding schemes, including spatial multiplexing (SM) [15]–[17], the error rate with any planar receive array decays no faster than SNR^{-3} even though the channel is purely LoS and experiences no fading (see Section III).

We consider the smallest number of receive antennas $n_r = 4$ that can form a 3-D, i.e., nonplanar, arrangement, and derive bounds on error performance when they form a tetrahedral array. In this case, the error probability decays faster than that of a rank 1 channel and is always exponential in SNR irrespective of the coding scheme used (see Section IV-A). We then design a LoS MIMO system with a good error performance for all transmit and receive array orientations over a range of interterminal distances by using a tetrahedral receive array and adaptively choosing two transmit antennas from a triangular/pentagonal array at the transmitter (see Section IV-B). Finally, we present simulation results to support our theoretical claims (see Section V).

Notation: Matrices and column vectors are denoted by bold upper-case and lower-case symbols, respectively. The symbols $\mathbf{A}^{\mathsf{T}}$, $\mathbf{A}^{\dagger}$, and $\|\mathbf{A}\|_F$ denote the transpose, the conjugate-transpose, and the Frobenius norm of a matrix $\mathbf{A}$. The symbol $\|\cdot\|$ denotes the 2-norm of a vector. For a complex number z, $\arg(z)$ and $\mathrm{Re}(z)$ denote its phase and real part, respectively. The expectation operator is denoted by $\mathbb{E}(\cdot)$.

II. $2 \times n_r$ LoS MIMO Channel

We consider MIMO LoS transmission with $n_t = 2$ antennas at the transmitter and $n_r \geq 2$ antennas at the receiver. Assuming that the large-scale fading effects, such as path loss, are accounted for in the link budget, we take the magnitude of the complex channel gain between any transmit–receive antenna pair to be unity. If $r_{m,n}$ is the distance between the nth transmit and the mth receive antennas, then the (m, n)th component of channel matrix $\mathbf{H} \in \mathbb{C}^{n_r \times 2}$ is [4]

$$h_{m,n} = \exp\left(i\frac{2\pi r_{m,n}}{\lambda}\right) \tag{1}$$

where λ is the carrier wavelength and $i = \sqrt{-1}$. The resulting wireless channel is $\mathbf{y}_{\mathsf{Rx}} = \sqrt{\mathsf{SNR}}\mathbf{H}\mathbf{x} + \mathbf{w}_{\mathsf{Rx}}$, where $\mathbf{y}_{\mathsf{Rx}} \in \mathbb{C}^{n_r}$ is the received vector, $\mathbf{x} \in \mathbb{C}^2$ is the transmitted vector, $\mathbf{w}_{\mathsf{Rx}} \in \mathbb{C}^{n_r}$ is the circularly symmetric complex white Gaussian noise with unit variance per complex dimension, and SNR is the SNR at each receive antenna. The power constraint at the transmitter is $\mathbb{E}\left(\|\mathbf{x}\|^2\right) \leq 1$. We assume that the channel matrix $\mathbf{H}$ is known at the receiver but not at the transmitter. Let $\mathbf{h}_1, \mathbf{h}_2 \in \mathbb{C}^{n_r}$ denote the two columns of $\mathbf{H}$, and $\mathbf{H} = \mathbf{QR}$ be its QR decomposition where $\mathbf{Q} \in \mathbb{C}^{n_r \times 2}$ has orthonormal columns, i.e., $\mathbf{Q}$ is a semi-unitary matrix, and

$$\mathbf{R} = \begin{bmatrix} \|\mathbf{h}_1\| & \dfrac{\mathbf{h}_1^{\dagger}\mathbf{h}_2}{\|\mathbf{h}_1\|} \\ 0 & \sqrt{\|\mathbf{h}_2\|^2 - \dfrac{\left|\mathbf{h}_1^{\dagger}\mathbf{h}_2\right|^2}{\|\mathbf{h}_1\|^2}} \end{bmatrix}.$$

Let μ denote the correlation between the two columns $\mathbf{h}_1$ and $\mathbf{h}_2$ of $\mathbf{H}$, and θ_μ be the phase of $\mathbf{h}_1^{\dagger}\mathbf{h}_2$, i.e.,

$$\mu = \frac{|\mathbf{h}_1^{\dagger}\mathbf{h}_2|}{\|\mathbf{h}_1\|\,\|\mathbf{h}_2\|} \text{ and } \theta_\mu = \arg\left(\mathbf{h}_1^{\dagger}\mathbf{h}_2\right).$$

From (1), we have $\|\mathbf{h}_1\| = \|\mathbf{h}_2\| = \sqrt{n_r}$, and hence

$$\mathbf{R} = \sqrt{n_r}\begin{bmatrix} 1 & \mathrm{e}^{i\theta_\mu}\mu \\ 0 & \sqrt{1-\mu^2} \end{bmatrix}. \tag{2}$$

Since $\mathbf{Q}$ is semi-unitary and $\mathbf{w}_{\mathsf{Rx}}$ is a white Gaussian noise vector, $\mathbf{y} = \mathbf{Q}^{\dagger}\mathbf{y}_{\mathsf{Rx}}$ is a sufficient statistic for $\mathbf{x}$. Hence, in the rest of the paper we will consider the following equivalent channel:

$$\mathbf{y} = \sqrt{\mathsf{SNR}}\mathbf{R}\mathbf{x} + \mathbf{w} \tag{3}$$

where $\mathbf{R}$ is given in (2), and $\mathbf{w} = \mathbf{Q}^{\dagger}\mathbf{x}$ is a 2-D circularly symmetric complex white Gaussian noise with zero mean and unit variance per complex dimension.

A. Modeling the $\mathbf{R}$ matrix

To analyze the error performance of arbitrary coding schemes in LoS MIMO channels, we model the phase θ_μ as independent of μ and uniformly distributed in $[0, 2\pi)$. Deriving the probability distribution of θ_μ and μ appears difficult; however, we provide an analytical motivation and numerical examples to support the validity of our model.

We follow the notations from [3] and [4] to describe the geometry of the transmit and receive antenna positions, as illustrated in Fig. 1.

We denote the interantenna distance at the transmitter by d_t, and define the origin O of the 3-D reference coordinate system as the midpoint between the two transmit antennas. Define the z-axis of the coordinate system to be along the line connecting

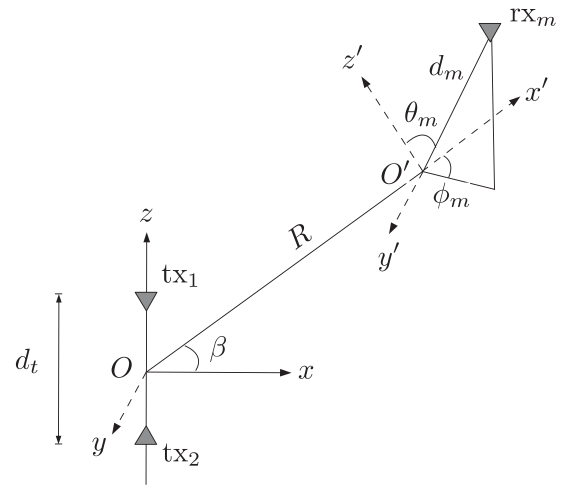

Fig. 1. Illustration of the parameters used in the system model.

the two transmit antennas, i.e., the positions of the two transmit antennas are $\left[0,\ 0,\ \frac{d_t}{2}\right]^\mathsf{T}$ and $\left[0,\ 0,\ -\frac{d_t}{2}\right]^\mathsf{T}$, respectively. Choose the x-axis of the coordinate system such that the centroid O' of the receive antenna array lies on the x–z plane. Let O' be at a distance of R from O and at an angle β to the x-axis, i.e., at the point $\left[R\cos\beta,\ 0,\ R\sin\beta\right]^\mathsf{T}$. Consider an auxiliary coordinate system with O' as the origin and the three axes x', y', z' defined as follows: the x' axis is along the direction OO', i.e., along the vector $\left[\cos\beta,\ 0,\ \sin\beta\right]^\mathsf{T}$, z' axis is on the x–z plane, and y' is parallel to y. Let (d_m, θ_m, ϕ_m) be the spherical coordinates of the mth receive antenna with respect to this auxiliary coordinate system, where d_m is the radial distance, θ_m is the polar angle, and ϕ_m is the azimuthal angle. The distance $r_{m,n}$ between the nth transmit and mth receive antennas satisfies [5][1]

$$r_{m,n} \approx R + d_m \sin\theta_m \cos\phi_m \ + (-1)^n \frac{d_t}{2}\sin\beta + \frac{(d_m\sin\theta_m\sin\phi_m)^2 + (d_m\cos\theta_m + (-1)^n \frac{d_t}{2}\cos\beta)^2}{2R}.$$

Therefore, the difference $r_{m,2} - r_{m,1}$ is given by

$$\begin{aligned} r_{m,2} - r_{m,1} &= d_t\sin\beta + \frac{(d_m\cos\theta_m + \frac{d_t}{2}\cos\beta)^2}{2R} \\ &\quad - \frac{(d_m\cos\theta_m - \frac{d_t}{2}\cos\beta)^2}{2R} \\ &= d_t\sin\beta + \frac{d_t d_m \cos\beta\cos\theta_m}{R}. \end{aligned} \tag{4}$$

[1]The angle β is equal to the parameter θ_t used in [3] and [4].

Let $F(\beta) = \mathbf{h}_1^\dagger\mathbf{h}_2$ denote the inner product between the two columns of $\mathbf{H}$ as a function of β. Using (1) and (4), we obtain

$$\begin{aligned} F(\beta) = \mathbf{h}_1^\dagger\mathbf{h}_2 &= \sum_{m=1}^{n_r} h_{m,1}^\dagger h_{m,2} \\ &= \exp\left(\frac{i2\pi d_t\sin\beta}{\lambda}\right)\sum_{m=1}^{n_r}\exp\left(\frac{i2\pi d_t d_m\cos\beta\cos\theta_m}{R\lambda}\right). \end{aligned} \tag{5}$$

Let $f_1(\beta) = \exp\left(i2\pi d_t\sin\beta/\lambda\right)$ and

$$f_2(\beta) = \sum_{m=1}^{n_r}\exp\left(\frac{i2\pi d_t d_m\cos\beta\cos\theta_m}{R\lambda}\right).$$

Then, $F(\beta) = f_1(\beta)f_2(\beta)$, $\arg F = \arg f_1 + \arg f_2$, and since $|f_1| = 1$, we also have $|F| = |f_2|$.

We now upper bound the magnitude of the derivative of μ with respect to β. The derivative of $\mathrm{d}f_2/\mathrm{d}\beta$ equals

$$\sum_{m=1}^{n_r}\frac{-i2\pi d_t d_m\sin\beta\cos\theta_m}{R\lambda}\exp\left(\frac{i2\pi d_t d_m\cos\beta\cos\theta_m}{R\lambda}\right). \tag{6}$$

Note that $|\mathrm{d}f_2/\mathrm{d}\beta| \le b$, where $b = \frac{2\pi d_t\sum_{m=1}^{n_r} d_m}{R\lambda}$. For an infinitesimal change $\Delta\beta$ in the value of β

$$|f_2(\beta+\Delta\beta)| - |f_2(\beta)| = \left|f_2(\beta) + \frac{\mathrm{d}f_2}{\mathrm{d}\beta}\Delta\beta\right| - |f_2(\beta)|.$$

Using the fact that $\big|\,|u+w| - |u|\,\big| \le |w|$ for any $u, w \in \mathbb{C}$, we have

$$\Big|\,|f_2(\beta+\Delta\beta)| - |f_2(\beta)|\,\Big| \le \left|\frac{\mathrm{d}f_2}{\mathrm{d}\beta}\right||\Delta\beta| \le b|\Delta\beta|.$$

It follows immediately that $|\,\mathrm{d}|f_2|/\mathrm{d}\beta\,| \le b$. Using the fact that $\mu = |F(\beta)|/n_r = |f_2(\beta)|/n_r$, we have

$$\left|\frac{\mathrm{d}\mu}{\mathrm{d}\beta}\right| = \frac{1}{n_r}\left|\frac{\mathrm{d}|f_2|}{\mathrm{d}\beta}\right| \le \frac{b}{n_r}. \tag{7}$$

Note that $\theta_\mu = \arg F = \arg f_1 + \arg f_2$, and hence, $\mathrm{d}\theta_\mu/\mathrm{d}\beta = \mathrm{d}(\arg f_1)/\mathrm{d}\beta + \mathrm{d}(\arg f_2)/\mathrm{d}\beta$. Now, $\arg f_1 = 2\pi d_t \sin\beta/\lambda$, and hence, $\mathrm{d}(\arg f_1)/\mathrm{d}\beta = 2\pi d_t\cos\beta/\lambda$. Using (7) and the fact that the range of transmission R is much larger than d_m, we have

$$\frac{\mathrm{d}(\arg f_1)}{\mathrm{d}\beta} = \frac{2\pi d_t\cos\beta}{\lambda} \gg \frac{2\pi d_t}{\lambda}\frac{\sum_{m=1}^{n_r} d_m}{R\,n_r} = \frac{b}{n_r} \ge \left|\frac{\mathrm{d}\mu}{\mathrm{d}\beta}\right|.$$

Hence, we expect $\mathrm{d}\theta_\mu/\mathrm{d}\beta \gg |\mathrm{d}\mu/\mathrm{d}\beta|$, i.e., a small change in the value of β, that causes a negligible change in μ, changes the phase θ_μ by an entire cycle of 2π rad. This motivates the channel model where θ_μ is independent of μ and uniformly distributed in the interval $[0, 2\pi)$.

Example 1: Consider a 2×2 LoS system operating in E-band at the frequency of 72 GHz over a distance $R = 10$ m. Let the two receive antennas be positioned such that $\theta_1 = 0$, $\theta_2 = \pi$, $\phi_1 = \phi_2 = 0$, and $d_1 = d_2 = d_r/2$. Then, using (5), we have

$$\mathbf{h}_1^\dagger\mathbf{h}_2 = 2\exp\left(\frac{i2\pi d_t\sin\beta}{\lambda}\right)\cos\left(\frac{\pi d_t d_r\cos\beta}{R\lambda}\right).$$

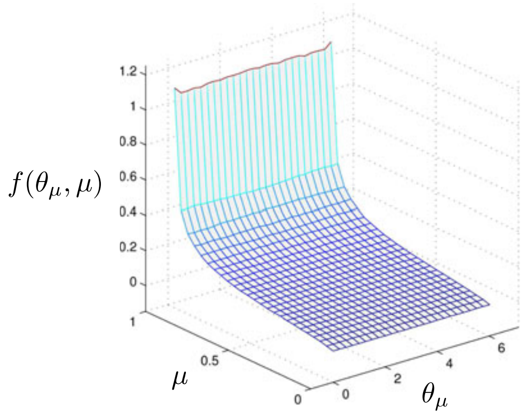

Fig. 2. Joint probability density function $f(\theta_\mu, \mu)$ of Example 2.

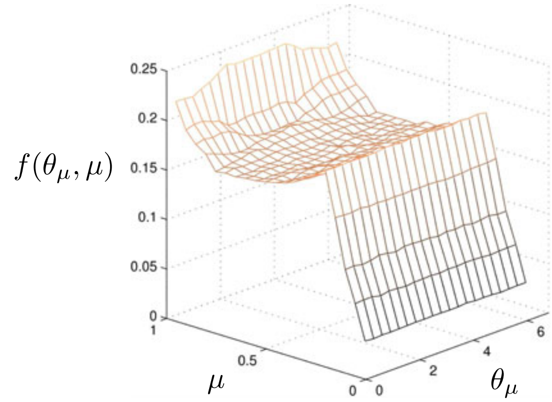

Fig. 3. Joint probability density function $f(\theta_\mu, \mu)$ of Example 3.

It follows that

$$\mu = \cos\left(\frac{\pi d_t d_r \cos\beta}{R\lambda}\right) \text{ and } \theta_\mu = \frac{2\pi d_t \sin\beta}{\lambda}. \tag{8}$$

Suppose the antenna geometry is to be configured so that $\mathbf{H}$ is unitary, i.e., $\mu = 0$, under the assumption that $\beta = 0$. This can be achieved by choosing d_t and d_r so that

$$\frac{d_t d_r \cos\beta}{R\lambda} = \frac{d_t d_r}{R\lambda} = \frac{1}{2}.$$

This is the criterion for uniform linear arrays (ULAs) given in [3]–[5]. With $\lambda = 4.2$ mm, the choice of $d_t = d_r = \sqrt{R\lambda/2} = 0.145$ m yields $\mu = 0$. With this choice of d_t and d_r, through direct computation using (8), we observe that as β undergoes a small variation in value from 0 through 0.029 rad (1.66°), the corresponding value of μ changes from 0 to 6.6×10^{-4}, while θ_μ ranges over the entire interval from 0 to 2π rad.

Example 2: Continuing with the 2×2 system of Example 1, now assume that the transmit and receive arrays are affected by independent random rotations about their respective centroids. The random rotations are uniformly distributed over the space of all 3-D rotations. The channel matrix $\mathbf{H}$ and the parameters θ_μ and μ are now random variables. The joint probability density function $f(\theta_\mu, \mu)$ obtained using Monte-Carlo methods is shown in Fig. 2 . We computed $f(\theta_\mu, \mu)$ over a rectangular grid of 625 points using 10^7 randomly generated instances of $\mathbf{H}$. For any fixed μ, we observe that $f(\theta_\mu, \mu)$ is essentially constant across all values of θ_μ, implying that θ_μ is uniformly distributed in $[0, 2\pi)$ and is independent of μ.

Example 3: Consider a 2×4 LoS MIMO system, with a rectangular array at the receiver, carrier frequency of 72 GHz, and interterminal distance of $R = 10$ m. The receive antennas are placed at the vertices of a square whose edges are of length d_r. We choose $d_t = d_r = \sqrt{R\lambda/2}$, which yields the ideal channel (i.e., $\mu = 0$) if the transmit and receive arrays are placed broadside to each other [5]. The joint probability density function $f(\theta_\mu, \mu)$, obtained using Monte-Carlo methods, when the transmit and receive arrays undergo uniformly random rotations about their centroids is shown in Fig. 3 . As in Example 2, the numerical result supports the validity of our channel model.

In the rest of the paper, we model the $2 \times n_r$ LoS channel using the 2×2 matrix [cf. (3)]

$$\mathbf{R} = \sqrt{n_r}\begin{bmatrix} 1 & e^{i\Theta}\mu \\ 0 & \sqrt{1-\mu^2} \end{bmatrix} \tag{9}$$

where Θ is uniformly distributed in $[0, 2\pi)$ and

$$\mu = \frac{1}{n_r}\left|\sum_{m=1}^{n_r} \exp\left(\frac{i2\pi d_t d_m \cos\beta\cos\theta_m}{R\lambda}\right)\right|. \tag{10}$$

B. Coding Schemes

We analyze the error performance of an arbitrary coding scheme for two transmit antennas with a finite transmission duration. Let $T \geq 1$ denote the transmission duration of a given communication scheme and $\mathscr{C} \subset \mathbb{C}^{2\times T}$ the finite set of all possible transmit codewords. The rows of the codewords $\mathbf{X} \in \mathscr{C}$ correspond to the two transmit antennas and the columns to the T time slots. All codewords are equally likely to be transmitted and the optimal decoder, i.e., the maximum-likelihood (ML) decoder, is used at the receiver. We further assume that the communication scheme satisfies the average power constraint $\sum_{\mathbf{X}\in\mathscr{C}} \|\mathbf{X}\|_F^2 \leq |\mathscr{C}|\, T$. Our analysis holds for arbitrary codes $\mathscr{C}$, including space-time block codes (STBCs) [18].

We now briefly recall two specific coding schemes that will be used in our simulations (in Section V) to illustrate our analytical results. *SM* [15]–[17], which is also known as *VBLAST* in the literature, is a simple yet powerful scheme wherein independent information symbols are transmitted across different antennas and time slots. The codebook $\mathscr{C} \subset \mathbb{C}^{2\times 1}$ corresponding to SM occupies $T = 1$ time slot, and is given by

$$\mathscr{C} = \left\{ \begin{bmatrix} s_1 \\ s_2 \end{bmatrix} \,\middle|\, s_1, s_2 \in \mathcal{A} \right\}$$

where $\mathcal{A}$ is a complex constellation, such as quadratic-amplitude modulation (QAM) or phase-shift keying.

The *Golden code* [19] is an STBC for two transmit antennas occupying $T = 2$ time slots, and is given by

$$\mathscr{C} = \left\{ \begin{bmatrix} \alpha(s_1 + \tau s_3) & \alpha(s_2 + \tau s_4) \\ i\bar{\alpha}(s_2 + \mu s_4) & \bar{\alpha}(s_1 + \mu s_3) \end{bmatrix} \,\middle|\, s_1, \ldots, s_4 \in \mathcal{A} \right\}$$

where $\mathcal{A}$ is a QAM constellation, $\tau = (1+\sqrt{5})/2$, $\mu = 1/\tau$, $\alpha = 1 + i\mu$, and $\bar{\alpha} = 1 + i\tau$. Unlike SM, the Golden code spreads the information symbols across time and antennas.

Both SM and Golden code have been well studied in the case of non-LoS MIMO fading channels. The SM scheme provides high data rate with low complexity encoding and decoding, while the Golden code provides high data rate, full-diversity as well as a large coding gain at the cost of higher decoding complexity in fading channels.

C. Error Probability Analysis for a Fixed μ

We now analyze the error performance of a given arbitrary coding scheme for a fixed value of μ. Let $\mathscr{C} \subset \mathbb{C}^{2\times T}$ be any code and $\mathbf{X}_a, \mathbf{X}_b \in \mathscr{C}$ be two distinct codewords. Let $\Delta\mathbf{X} = \mathbf{X}_a - \mathbf{X}_b$ be the pairwise codeword difference matrix. The pairwise error probability between $\mathbf{X}_a$ and $\mathbf{X}_b$ for a fixed μ and a given realization $\Theta = \theta$ is [18]

$$\mathsf{PEP}\left(\mathbf{X}_a \to \mathbf{X}_b | \mu, \Theta = \theta\right) = \mathcal{Q}\left(\sqrt{\frac{\mathsf{SNR}\|\mathbf{R}\Delta\mathbf{X}\|_F^2}{2}}\right)$$

where $\mathcal{Q}$ is the Gaussian tail function. Using the Chernoff bound $\mathcal{Q}(x) \le \frac{\exp\left(-x^2/2\right)}{2}$, we have the upper bound

$$\mathsf{PEP} \le \frac{1}{2}\exp\left(-\frac{\mathsf{SNR}}{4}\|\mathbf{R}\Delta\mathbf{X}\|_F^2\right). \tag{11}$$

Denoting the two rows of the matrix $\Delta\mathbf{X}$ as $\Delta\mathbf{x}_1^{\mathsf{T}}$ and $\Delta\mathbf{x}_2^{\mathsf{T}}$, we obtain the following expression for the squared Euclidean distance between the codewords at the receiver:

$$\begin{aligned}\|\mathbf{R}\Delta\mathbf{X}\|_F^2 &= n_r\left(\|\Delta\mathbf{x}_1\|^2 + \|\Delta\mathbf{x}_2\|^2 + 2\mu\,\mathrm{Re}(\mathrm{e}^{i\theta}\Delta\mathbf{x}_1^{\dagger}\Delta\mathbf{x}_2)\right)\\ &= n_r\left(\|\Delta\mathbf{x}_1\|^2 + \|\Delta\mathbf{x}_2\|^2 + 2\mu\cos\theta'|\Delta\mathbf{x}_1^{\dagger}\Delta\mathbf{x}_2|\right)\end{aligned} \tag{12}$$

where $\theta' = \theta + \arg(\Delta\mathbf{x}_1^{\dagger}\Delta\mathbf{x}_2) \bmod 2\pi$.

1) Worst-Case Error Probability Over θ: For a given μ, the value of θ that minimizes the squared Euclidean distance $\|\mathbf{R}\Delta\mathbf{X}\|^2$ at the receiver is $\theta^* = \pi + \arg(\Delta\mathbf{x}_1^{\dagger}\Delta\mathbf{x}_2)$ since it leads to $\cos\theta' = -1$ in (12). Using the notation

$$d(\mu, \Delta\mathbf{X}) = \|\Delta\mathbf{x}_1\|^2 + \|\Delta\mathbf{x}_2\|^2 - 2\mu|\Delta\mathbf{x}_1^{\dagger}\Delta\mathbf{x}_2| \tag{13}$$

the worst-case squared Euclidean distance is

$$\min_{\theta\in[0,2\pi)} \|\mathbf{R}\Delta\mathbf{X}\|_F^2 = n_r d(\mu, \Delta\mathbf{X}).$$

Thus, the worst-case PEP for a fixed μ satisfies

$$\mathsf{PEP}^*(\mu) \le \frac{1}{2}\exp\left(\frac{-n_r\,\mathsf{SNR}\,d(\mu,\Delta\mathbf{X})}{4}\right). \tag{14}$$

2) Average Error Probability Over Θ: Since Θ is uniformly distributed in $[0, 2\pi)$, so is $\Theta' = \Theta + \arg(\Delta\mathbf{x}_1^{\dagger}\Delta\mathbf{x}_2) \bmod 2\pi$. Using (11) and (12), the error probability averaged over Θ, for a fixed μ, can be upper bounded as follows:

$$\begin{aligned}\mathbb{E}_\Theta\left(\mathsf{PEP}\right) &\le \mathbb{E}_\Theta\left(\frac{1}{2}\exp\left(-\frac{\mathsf{SNR}}{4}\|\mathbf{R}\Delta\mathbf{X}\|_F^2\right)\right)\\ &= \frac{1}{2}\exp\left(\frac{-\mathsf{SNR}n_r\left(\|\Delta\mathbf{x}_1\|^2 + \|\Delta\mathbf{x}_2\|^2\right)}{4}\right)\\ &\quad\times\frac{1}{2\pi}\int_0^{2\pi}\exp\left(-\frac{\mathsf{SNR}n_r}{4}2\mu\cos\theta'|\Delta\mathbf{x}_1^{\dagger}\Delta\mathbf{x}_2|\right)\mathrm{d}\theta'\\ &= \frac{1}{2}\exp\left(\frac{-\mathsf{SNR}n_r\left(\|\Delta\mathbf{x}_1\|^2 + \|\Delta\mathbf{x}_2\|^2\right)}{4}\right)\\ &\quad\times\ I_0\left(\frac{\mathsf{SNR}n_r}{2}\mu|\Delta\mathbf{x}_1^{\dagger}\Delta\mathbf{x}_2|\right)\end{aligned}$$

where

$$\begin{aligned}I_0(x) &= \frac{1}{\pi}\int_0^{\pi}\exp\left(x\cos\theta'\right)\mathrm{d}\theta' = \frac{1}{2\pi}\int_0^{2\pi}\exp\left(x\cos\theta'\right)\mathrm{d}\theta'\\ &= \frac{1}{2\pi}\int_0^{2\pi}\exp\left(-x\cos\theta'\right)\mathrm{d}\theta'\end{aligned}$$

is the modified Bessel function of the first kind and zeroth order. For large x, we have [20]

$$I_0(x) = \frac{\mathrm{e}^x}{\sqrt{2\pi x}}\left(1 + O\left(x^{-1}\right)\right). \tag{15}$$

Using (13) and the first-order approximation (15), we get the following approximate upper bound when $\mu > 0$:

$$\begin{aligned}\mathbb{E}_\Theta\left(\mathsf{PEP}\right) \lesssim &\frac{1}{\sqrt{4\pi n_r\mathsf{SNR}\mu|\Delta\mathbf{x}_1^{\dagger}\Delta\mathbf{x}_2|}}\\ &\times\ \exp\left(-\frac{n_r\mathsf{SNR}}{4}d(\mu,\Delta\mathbf{X})\right).\end{aligned} \tag{16}$$

Since the exponential function decays more rapidly than $\mathsf{SNR}^{-1/2}$, the high SNR behavior is dictated by $d(\mu, \Delta\mathbf{X})$.

In this section, we derived bounds on PEP for a fixed μ. In Sections III and IV, we analyze the effects of random rotations of the terminals on μ and error performance.

III. Error Performance of Planar Receive Arrays

Assume that the receive antenna system is affected by a random 3-D rotation $\mathbf{U} \in \mathbb{R}^{3\times 3}$ about its centroid O'. Let the rotation $\mathbf{U}$ be uniformly distributed on the set of all 3-D rotations, i.e., the special orthogonal group

$$\mathrm{SO}_3 = \left\{\mathbf{U} \in \mathbb{R}^{3\times 3}\,|\,\mathbf{U}\mathbf{U}^{\mathsf{T}} = \mathbf{I}, \det(\mathbf{U}) = 1\right\}.$$

In Theorem 1, we provide a lower bound on the average pairwise error probability over a LoS MIMO channel with a planar receive array. To do so, we derive a lower bound on the probability that a random rotation $\mathbf{U}$ would lead to a "bad" channel matrix with μ close to 1, i.e., $\mu \ge 1 - \epsilon$ for some small positive ϵ. By analyzing the PEP for this class of bad channels, and letting ϵ decay suitably with SNR, we arrive at a lower bound for the average PEP at high SNR.

Theorem 1: Let the receive antenna array be any planar arrangement of n_r antennas, $n_r \geq 2$, undergoing a uniformly distributed random rotation $\mathbf{U}$ about its centroid. At high SNR, for any transmit orientation β, we have

$$\mathbb{E}(\mathsf{PEP}) \geq \frac{\exp\left(-\frac{n_r \,\mathrm{c}\, |\Delta\mathbf{x}_1^\dagger \Delta\mathbf{x}_2|}{2}\right)}{2n_r \mathsf{SNR}^3 \sqrt{2\pi^2 |\Delta\mathbf{x}_1^\dagger \Delta\mathbf{x}_2|} \left(\|\Delta\mathbf{X}\|_F + \frac{1}{\sqrt{n_r \mathsf{SNR}}}\right)} \times \exp\left(-\frac{n_r \mathsf{SNR}}{4} d(1, \Delta\mathbf{X})\right) \quad (17)$$

where $\mathrm{c} = \max_{m=1}^{n_r} 2\pi d_t d_m / R\lambda$.

Proof: Let $\{\mathbf{e}_x, \mathbf{e}_y, \mathbf{e}_z\}$ be the standard basis in $\mathbb{R}^3$. When the receive system undergoes no rotation, i.e., when $\mathbf{U} = \mathbf{I}$, let the position of the mth receive antenna relative to the centroid O' of the receive antenna system be $d_m \mathbf{r}_m$, where $\mathbf{r}_m \in \mathbb{R}^3$ is a unit vector. Since the receive array is planar and the random rotation $\mathbf{U}$ is uniformly distributed, without loss of generality, we assume that the vectors $\mathbf{r}_1, \ldots, \mathbf{r}_{n_r}$ are in the linear span of $\mathbf{e}_x$ and $\mathbf{e}_z$. From Fig. 1, we see that θ_m in (5) is the angle between the orientation $\mathbf{U}\mathbf{r}_m$ of the mth receiver and the unit vector $\tilde{\mathbf{v}} = \left[-\sin\beta,\, 0,\, \cos\beta\right]^\mathsf{T}$ along z'-axis, i.e., $\cos\theta_m = \mathbf{r}_m^\mathsf{T} \mathbf{U}^\mathsf{T} \tilde{\mathbf{v}}$. Note that $\mathbf{U}^\mathsf{T}$ has the same distribution as $\mathbf{U}$, and $\mathbf{v} = \mathbf{U}^\mathsf{T} \tilde{\mathbf{v}}$ is uniformly distributed on the unit sphere in $\mathbb{R}^3$. The resulting random variable $|\mathbf{e}_y^\mathsf{T} \mathbf{v}|$ is known to be uniformly distributed in the interval $[0, 1]$.

For a small positive number $\delta > 0$, consider the event $\mathcal{E}$: $|\mathbf{e}_y^\mathsf{T} \mathbf{v}|^2 \geq 1 - \delta^2$. The probability of $\mathcal{E}$ is

$$P(\mathcal{E}) = P\left(|\mathbf{e}_y^\mathsf{T} \mathbf{v}| \geq \sqrt{1 - \delta^2}\right) = 1 - \sqrt{1 - \delta^2} \approx \frac{\delta^2}{2}$$

for small values of δ. We will now derive an upper bound for the PEP for the case when $\mathcal{E}$ is true. Using the following inequalities, we first show that $|\cos\theta_m| \leq \delta$, for all $m = 1, \ldots, n_r$

$$\begin{aligned} |\cos\theta_m|^2 &= |\mathbf{r}_m^\mathsf{T} \mathbf{v}|^2 \\ &\leq |\mathbf{e}_x^\mathsf{T} \mathbf{v}|^2 + |\mathbf{e}_z^\mathsf{T} \mathbf{v}|^2 \text{ (since } \mathbf{r}_m \in \operatorname{span}(\mathbf{e}_x, \mathbf{e}_z)) \\ &= \|\mathbf{v}\|^2 - |\mathbf{e}_y^\mathsf{T} \mathbf{v}|^2 \\ &\leq 1 - (1 - \delta^2) = \delta^2. \end{aligned}$$

Let $c_m = 2\pi d_t d_m \cos\beta / R\lambda$ and $c_{\max} = \max\{c_1, \ldots, c_{n_r}\}$. From (10), we have

$$\mu = \frac{1}{n_r} \left| \sum_{m=1}^{n_r} \exp\left(i c_m \cos\theta_m\right) \right|.$$

We will now show that the value of μ is close to 1 when $\mathcal{E}$ is true. If $\epsilon_m = 1 - \exp(i c_m \cos\beta)$, then

$$\begin{aligned} |\epsilon_m|^2 &= (1 - \cos(c_m \cos\theta_m))^2 + \sin^2(c_m \cos\theta_m) \\ &= 2 - 2\cos(c_m \cos\theta_m) \\ &\approx 2 - 2\left(1 - \frac{c_m^2 \cos^2(\theta_m)}{2}\right) \\ &= c_m^2 \cos^2(\theta_m) \leq \delta^2 c_{\max}^2 \end{aligned}$$

where the approximation follows from Taylor's series expansion of the $\cos(\cdot)$ function and the fact that $|c_m \cos\theta_m| \leq c_m \delta$ is small. Now

$$\begin{aligned} \mu &= \frac{1}{n_r} \left| \sum_1^{n_r} (1 - \epsilon_m) \right| = \frac{1}{n_r} \left| n_r - \sum_1^{n_r} \epsilon_m \right| \\ &\geq 1 - \frac{1}{n_r} \sum_1^{n_r} |\epsilon_m| \geq 1 - \delta c_{\max}. \end{aligned}$$

Thus, $\mu \geq 1 - \delta c_{\max}$ whenever $\mathcal{E}$ is true.

The pairwise error probability for fixed μ and $\Theta = \theta$ is $\mathcal{Q}(\sqrt{\mathsf{SNR} \|\mathbf{R}\Delta\mathbf{X}\|_F^2 / 2})$. Since we need a lower bound on the probability of error, we use the following lower bound for the Gaussian tail function [21]:

$$\mathcal{Q}(x) \geq \frac{2}{\sqrt{2\pi}\left(x + \sqrt{x^2 + 4}\right)} \exp\left(-\frac{x^2}{2}\right), \text{ for } x \geq 0.$$

Using $x^2 + 4 \leq (x + 2)^2$ for $x \geq 0$, we obtain a more relaxed bound

$$\mathcal{Q}(x) \geq \frac{1}{\sqrt{2\pi}(x + 1)} \exp\left(-\frac{x^2}{2}\right).$$

In our case $x = \sqrt{\mathsf{SNR} \|\mathbf{R}\Delta\mathbf{X}\|_F^2 / 2}$, and we use the exact value of x from (12) for the exponent, and the following upper bound for the denominator:

$$\begin{aligned} x &= \sqrt{\frac{\mathsf{SNR}}{2}} \|\mathbf{R}\Delta\mathbf{X}\|_F \leq \sqrt{\frac{\mathsf{SNR}}{2}} \|\mathbf{R}\|_F \; \|\Delta\mathbf{X}\|_F \\ &= \sqrt{n_r \mathsf{SNR}} \|\Delta\mathbf{X}\|_F. \end{aligned}$$

Thus, we have the following lower bound for a fixed μ and $\Theta = \theta$:

$$\mathsf{PEP} \geq \frac{\exp\left(-\frac{\mathsf{SNR}}{4} \|\mathbf{R}\Delta\mathbf{X}\|_F^2\right)}{\sqrt{2\pi}\left(\sqrt{n_r \mathsf{SNR}} \|\Delta\mathbf{X}\|_F + 1\right)}. \quad (18)$$

Since the denominator is independent of the phase Θ, we can use the same method as in Section II-C2 to obtain the average of the above lower bound over the uniformly distributed random variable Θ. Averaging (18) over Θ and using the approximation to the Bessel function (15), we obtain

$$\mathbb{E}_\Theta(\mathsf{PEP}) \gtrsim \frac{\exp\left(-\frac{n_r \mathsf{SNR}}{4} d(\mu, \Delta\mathbf{X})\right)}{n_r \mathsf{SNR} \sqrt{2\pi^2 \mu |\Delta\mathbf{x}_1^\dagger \Delta\mathbf{x}_2|} \left(\|\Delta\mathbf{X}\|_F + \frac{1}{\sqrt{n_r \mathsf{SNR}}}\right)}.$$

Using the trivial upper bound $\mu \leq 1$ in the denominator

$$\mathbb{E}_\Theta\,(\mathsf{PEP}) \gtrsim \frac{\exp\left(-\frac{n_r \mathsf{SNR}}{4} d(\mu, \Delta\mathbf{X})\right)}{n_r \mathsf{SNR} \sqrt{2\pi^2 |\Delta\mathbf{x}_1^\dagger \Delta\mathbf{x}_2|} \left(\|\Delta\mathbf{X}\|_F + \frac{1}{\sqrt{n_r \mathsf{SNR}}}\right)}. \quad (19)$$

Since $d(\mu, \Delta\mathbf{X})$ is a decreasing function of μ, if $\mathcal{E}$ is true, the numerator in the right-hand side of (19) can be lower bounded by $\exp(-\frac{n_r \mathsf{SNR}}{4} d(1 - \delta c_{\max}, \Delta\mathbf{X}))$. The expression (19) is a lower bound on the average PEP for a given μ. We now derive a lower bound for the PEP when averaged over both μ and Θ

as follows:

$$\begin{aligned}\mathbb{E}(\mathsf{PEP}) &= P(\mathcal{E})P\left(\mathbf{X}_a \to \mathbf{X}_b|\mathcal{E}\right) + P(\mathcal{E}^c)P\left(\mathbf{X}_a \to \mathbf{X}_b|\mathcal{E}^c\right)\\ &\geq P(\mathcal{E})P\left(\mathbf{X}_a \to \mathbf{X}_b|\mathcal{E}\right)\\ &\geq \frac{\delta^2 \exp\left(-\frac{n_r \mathsf{SNR}}{4} d(1-\delta c_{\max}, \Delta\mathbf{X})\right)}{2n_r \mathsf{SNR}\sqrt{2\pi^2|\Delta\mathbf{x}_1^\dagger \Delta\mathbf{x}_2|}\left(\|\Delta\mathbf{X}\|_F + \frac{1}{\sqrt{n_r \mathsf{SNR}}}\right)}.\end{aligned} \tag{20}$$

From the definition (13) of $d(\mu, \Delta\mathbf{X})$, we have

$$d(1-\delta c_{\max}, \Delta\mathbf{X}) = d(1, \Delta\mathbf{X}) + 2\delta c_{\max}|\Delta\mathbf{x}_1^\dagger \Delta\mathbf{x}_2|.$$

Using the above relation and choosing $\delta = \mathsf{SNR}^{-1}$, which is small for high SNR, we obtain

$$\mathbb{E}(\mathsf{PEP}) \geq \frac{\exp\left(-\frac{n_r c_{\max}|\Delta\mathbf{x}_1^\dagger \Delta\mathbf{x}_2|}{2}\right)\exp\left(-\frac{n_r \mathsf{SNR}}{4} d(1, \Delta\mathbf{X})\right)}{2n_r \mathsf{SNR}^3\sqrt{2\pi^2|\Delta\mathbf{x}_1^\dagger \Delta\mathbf{x}_2|}\left(\|\Delta\mathbf{X}\|_F + \frac{1}{\sqrt{n_r \mathsf{SNR}}}\right)}.$$

Using $\cos\beta \leq 1$ in $c_m = 2\pi d_t d_m \cos\beta / R\lambda$ we obtain $c_{\max} \geq \max_m 2\pi d_t d_m / R_{\min}\lambda$. This completes the proof. ■

We compare the lower bound (17) on PEP for planar receive arrays undergoing random rotations, with the upper bound (16) for a channel with fixed $\mu = 1$. The dominant term dictating the rate of decay of error probability for both these channels is $\exp(-\frac{n_r \mathsf{SNR}}{4}\min_{\Delta\mathbf{X}} d(1, \Delta\mathbf{X}))$, where the minimization is over all nonzero codewords difference matrices $\Delta\mathbf{X} = \mathbf{X}_a - \mathbf{X}_b$ of the code $\mathscr{C}$. Note that $\mu = 1$ minimizes the performance metric $d(\mu, \Delta\mathbf{X})$, and corresponds to the worst-case scenario in which both $\mathbf{H}$ and $\mathbf{R}$ have rank 1. While planar receive arrays, such as the well-studied linear, rectangular, and circular arrays, provide an array gain (an n_r-fold increase in received SNR), their *asymptotic coding gain* $\min_{\Delta\mathbf{X}} d(1, \Delta\mathbf{X})$ provides no improvement over that of any rank 1 channel.

Theorem 1 further implies that when $\min_{\Delta\mathbf{X}} d(1, \Delta\mathbf{X}) = 0$, the error probability is no more exponential in SNR but decays at the most as fast as SNR^{-3}. Hence, although the channel is purely LoS and experiences no fading, the error performance with a planar arrangement of antennas can decay slowly, similar to a fading channel.

The parameter $d(1, \Delta\mathbf{X})$ satisfies the following tight inequality:

$$\begin{aligned} d(1, \Delta\mathbf{X}) &= \|\Delta\mathbf{x}_1\|^2 + \|\Delta\mathbf{x}_2\|^2 - 2|\Delta\mathbf{x}_1^\dagger \Delta\mathbf{x}_2|\\ &\geq \|\Delta\mathbf{x}_1\|^2 + \|\Delta\mathbf{x}_2\|^2 - 2\|\Delta\mathbf{x}_1\|\,\|\Delta\mathbf{x}_2\|\\ &= \left(\,\|\Delta\mathbf{x}_1\| - \|\Delta\mathbf{x}_2\|\,\right)^2. \end{aligned} \tag{21}$$

The second line follows from the Cauchy–Schwarz inequality, which is tight if and only if $\Delta\mathbf{x}_1$ and $\Delta\mathbf{x}_2$ are linearly dependent. Thus, $d(1, \Delta\mathbf{X}) = 0$ if and only if $\Delta\mathbf{x}_1$ and $\Delta\mathbf{x}_2$ are linearly dependent and $\|\Delta\mathbf{x}_1\| = \|\Delta\mathbf{x}_2\|$, i.e., if and only if $\Delta\mathbf{x}_1 = \alpha\Delta\mathbf{x}_2$ for some complex number α of unit magnitude. We use this observation in Example 4 to show that the widely used SM coding scheme suffers from such a slowly decaying error probability with planar receive arrays.

Example 4: Performance of spatial multiplexing with planar receive array. The codeword difference matrices of the SM scheme are of the form

$$\Delta\mathbf{X} = \begin{bmatrix}\Delta s_1\\ \Delta s_2\end{bmatrix}$$

where $\Delta s_1, \Delta s_2 \in \Delta\mathcal{A}$ and $\Delta\mathcal{A} = \{x - y \,|\, x, y \in \mathcal{A}\}$ is the set of pairwise differences of the complex constellation $\mathcal{A}$. When $\Delta s_1 = \Delta s_2$, the two rows of the codeword difference matrix $\Delta\mathbf{X}$ are equal resulting in $d(1, \Delta\mathbf{X}) = 0$. Hence, for the SM scheme, $\min_{\Delta\mathbf{X}} d(1, \Delta\mathbf{X}) = 0$, and from Theorem 1, the rate of decay of the average error probability will be no faster than SNR^{-3}. Note that this result is valid for any number of antennas n_r used in any planar arrangement of the receive array. This theoretical result is validated by our simulations (see Figs. 10 and 13) in Section V.

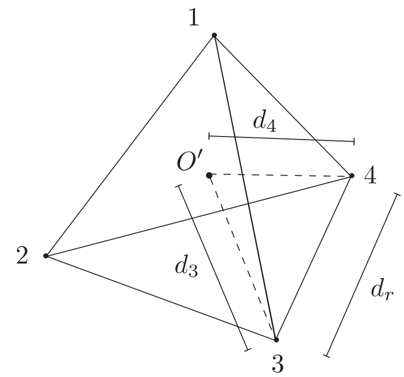

Fig. 4. Receive antennas are placed at the vertices $1, \ldots, 4$ of the tetrahedron. Also shown in the figure are the centroid O', the distances d_3 and d_4 of the antennas 3 and 4 from O', and the interantenna distance d_r.

IV. Error Performance of Tetrahedral Receive Array

The smallest number of antennas that can form a nonplanar arrangement is 4. In this section, we consider the case wherein $n_r = 4$ receive antennas are placed at the vertices of a regular tetrahedron (see Fig. 4). The interantenna distance d_r is the same for any pair of receive antennas, and this is related to the distance d_m of each antenna from the centroid O' of the receive array as $d_m = \sqrt{3/8}\, d_r$, $m = 1, \ldots, 4$. Let us define the *deviation factor* η as in [3] and [4] as follows:

$$\eta = \frac{R\lambda}{2d_t d_r \cos\beta}. \tag{22}$$

In the case of a tetrahedral receiver, using (10) and (22)

$$\mu = \frac{1}{4}\left|\sum_{m=1}^{4}\exp\left(i\frac{\pi}{\eta}\sqrt{\frac{3}{8}}\cos\theta_m\right)\right|.$$

The parameter η captures both the distance R and the transmit orientation β, while the variables $\theta_1, \ldots, \theta_4$ jointly determine the receive orientation $\mathbf{U}$. To upper bound the error probability using (14), we need the maximum value of μ over all possible η and $\mathbf{U}$. Let

$$\mu^*(\eta) = \max_{\mathbf{U}\in \mathrm{SO}_3}\frac{1}{4}\left|\sum_{m=1}^{4}\exp\left(i\frac{\pi}{\eta}\sqrt{\frac{3}{8}}\cos\theta_m\right)\right| \tag{23}$$

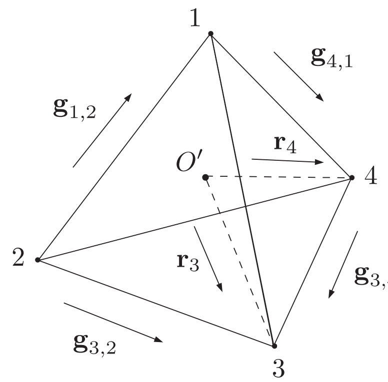

Fig. 5. Tetrahedron arrangement illustrating the vertices $1, \ldots, 4$, the reference O' at the centroid of the tetrahedron, and the directions of a few of the unit vectors $\mathbf{r}_m$ and $\mathbf{g}_{m,\ell}$.

be the maximum channel correlation over all receive orientations as a function of η. If one is aware of the range of values that R and β may assume, then one can upper bound the worst-case PEP using (14) as

$$\begin{aligned} \mathsf{PEP}^* &\leq \frac{1}{2}\exp\left(-\frac{n_r\,\mathsf{SNR}}{4}\, d(\max_{\eta}\mu^*(\eta), \Delta\mathbf{X})\right) \\ &= \frac{1}{2}\exp\left(-\mathsf{SNR}\; d(\max_{\eta}\mu^*(\eta), \Delta\mathbf{X})\right). \end{aligned} \tag{24}$$

A. Upper Bound on $\mu^*(\eta)$

In this section, we derive an upper bound on $\mu^*(\eta)$ for all $\eta \geq 1$. This result will allow us to show that the high SNR error performance of the tetrahedral array is better than any planar receive array when $\eta \geq 1$, and the receiver undergoes a uniformly random rotation. To derive this upper bound, we first show that when $\eta \geq 1$, irrespective of the receive array orientation, the 4×2 channel matrix $\mathbf{H}$ contains at least one 2×2 submatrix $\mathbf{H}_{\rm sub}$ such that the correlation $\mu_{\rm sub}$ between the two columns of $\mathbf{H}_{\rm sub}$ is at the most $\cos(\pi/2\sqrt{2}\eta)$. This latter problem is equivalent to finding the maximum distortion when a unit vector in $\mathbb{R}^3$ is quantized using a codebook $\mathcal{G}$ consisting of 12 unit vectors that correspond to the six edges of the tetrahedron along with the polarities ± 1. The computation of this maximum distortion is then simplified by showing that $\mathcal{G}$ is a *group code* [22].

We first introduce some notation to capture the geometrical properties of the tetrahedral array. Consider the tetrahedron shown in Fig. 5 with the centroid O'. Let $\mathbf{r}_m \in \mathbb{R}^3$ be the unit vector in the direction of the mth receive antenna with respect to the reference O'. Hence, the position vector of the mth receive antenna is $d_m\mathbf{r}_m$. If one applies a 3-D rotation $\mathbf{U} \in \mathbb{R}^{3\times 3}$ on the receive system about O', the position of the mth receive antenna is $d_m\mathbf{U}\mathbf{r}_m$. It is straightforward to show that the polar angle θ_m of the mth rotated receive antenna (cf. Fig. 1) satisfies $\cos\theta_m = \mathbf{r}_m^{\mathsf{T}}\mathbf{U}^{\mathsf{T}}\tilde{\mathbf{v}}$, where the unit vector $\tilde{\mathbf{v}} = \left[-\sin\beta,\, 0,\, \cos\beta\right]^{\mathsf{T}}$. Since $\mathbf{U}$ is an arbitrary rotation matrix, the set of all possible values assumed by the vector $\mathbf{v} = \mathbf{U}^{\mathsf{T}}\tilde{\mathbf{v}}$ is the sphere $\mathbb{S}^2$ consisting of all unit vectors in $\mathbb{R}^3$.

From (10), the correlation μ for a tetrahedral receiver is

$$\mu = \frac{1}{4}\left|\sum_{m=1}^{4}\exp\left(\frac{i2\pi d_t d_m\cos\beta\cos\theta_m}{R\lambda}\right)\right|$$

where $\cos\theta_m = \mathbf{r}_m^{\mathsf{T}}\mathbf{U}^{\mathsf{T}}\tilde{\mathbf{v}} = \mathbf{r}_m^{\mathsf{T}}\mathbf{v}$, and $\mathbf{v} \in \mathbb{S}^2$ captures the effect of the rotation undergone by the receive array. For any $m \neq \ell$, the unit vectors $\mathbf{r}_m$ and $\mathbf{r}_\ell$ satisfy $\|\mathbf{r}_m - \mathbf{r}_\ell\| = \sqrt{8/3}$. Let

$$\mathbf{g}_{m,\ell} = \frac{\mathbf{r}_m - \mathbf{r}_\ell}{\|\mathbf{r}_m - \mathbf{r}_\ell\|} = \sqrt{\frac{3}{8}}\,(\mathbf{r}_m - \mathbf{r}_\ell)$$

be the unit vector along $\mathbf{r}_m - \mathbf{r}_\ell$, i.e., along the edge of the tetrahedron between the vertices m and ℓ (see Fig. 5).

Let $\mathbf{H}_{\rm sub}$ be the 2×2 submatrix of $\mathbf{H}$ formed using the mth and ℓth rows. Note that $\mathbf{H}_{\rm sub}$ is the channel response seen through the receive antennas m and ℓ. Using the fact that $d_m = d_\ell = \sqrt{3/8}\,d_r$, the correlation between the columns of $\mathbf{H}_{\rm sub}$ can be written as

$$\begin{aligned} \mu_{\rm sub} &= \frac{1}{2}\Bigg|\exp\left(\frac{i2\pi d_t d_m\cos\beta\,\mathbf{r}_m^{\mathsf{T}}\mathbf{v}}{R\lambda}\right) \\ &\qquad + \exp\left(\frac{i2\pi d_t d_\ell\cos\beta\,\mathbf{r}_\ell^{\mathsf{T}}\mathbf{v}}{R\lambda}\right)\Bigg| \\ &= \frac{1}{2}\left|1 + \exp\left(\frac{i2\pi d_t d_m\cos\beta(\mathbf{r}_m - \mathbf{r}_\ell)^{\mathsf{T}}\mathbf{v}}{R\lambda}\right)\right| \\ &= \frac{1}{2}\left|1 + \exp\left(\frac{i2\pi d_t d_m\sqrt{8/3}\,\cos\beta\,\mathbf{g}_{m,\ell}^{\mathsf{T}}\mathbf{v}}{R\lambda}\right)\right| \\ &= \frac{1}{2}\left|1 + \exp\left(i\frac{\pi}{\eta}\,\mathbf{g}_{m,\ell}^{\mathsf{T}}\mathbf{v}\right)\right| \\ &= \left|\cos\left(\frac{\pi}{2\eta}\,\mathbf{g}_{m,\ell}^{\mathsf{T}}\mathbf{v}\right)\right| \end{aligned} \tag{25}$$

where the fourth equality follows from (22), and the last equality uses straightforward algebraic manipulations. Given an "orientation" $\mathbf{v}$, we intend to find the submatrix $\mathbf{H}_{\rm sub}$ with the least correlation $\mu_{\rm sub}$. If $\eta \geq 1$, we have

$$\left|\frac{\pi}{2\eta}\,\mathbf{g}_{m,\ell}^{\mathsf{T}}\mathbf{v}\right| \leq \frac{\pi}{2}.$$

Since cos is decreasing function in the interval $[0, \pi/2]$, from (25), the problem of finding $\mu_{\rm sub}$ translates to finding the edge $\mathbf{g}_{m,\ell}$ of the tetrahedron that has the largest inner product with $\mathbf{v}$.

We will now show that for any $\mathbf{v} \in \mathbb{S}^2$ there exists a $\mathbf{g}_{m,\ell}$ such that $\sqrt{1/2} \leq \mathbf{g}_{m,\ell}^{\mathsf{T}}\mathbf{v} \leq 1$. Since

$$\|\mathbf{v} - \mathbf{g}_{m,\ell}\|^2 = \|\mathbf{v}\|^2 + \|\mathbf{g}_{m,\ell}\|^2 - 2\,\mathbf{g}_{m,\ell}^{\mathsf{T}}\mathbf{v} = 2\Big(1 - \mathbf{g}_{m,\ell}^{\mathsf{T}}\mathbf{v}\Big)$$

this is equivalent to finding the maximum squared Euclidean error when the set of vectors $\mathcal{G} = \{\mathbf{g}_{m,\ell} \,|\, m \neq \ell\}$ is used as a codebook for quantizing an arbitrary unit vector $\mathbf{v}$ in $\mathbb{R}^3$. The set $\mathcal{G}$ contains 12 vectors, corresponding to the six edges of the tetrahedron together with the polarity ± 1.

Proposition 1: For any $\mathbf{v} \in \mathbb{S}^2$, there exist $m, \ell \in \{1, 2, 3, 4\}$, $m \neq \ell$, such that $\mathbf{g}_{m,\ell}^{\mathsf{T}}\mathbf{v} \geq \sqrt{1/2}$.

Proof: With some abuse of notation, we will denote the elements of $\mathcal{G}$ as $\mathbf{g}_1, \ldots, \mathbf{g}_{12}$. For each $i = 1, \ldots, 12$, let

$$\mathcal{D}_i = \left\{ \mathbf{v} \in \mathbb{S}^2 \,|\, \mathbf{g}_i^\mathsf{T} \mathbf{v} \geq \mathbf{g}_j^\mathsf{T} \mathbf{v}, \text{ for all } j \neq i \right\} \tag{26}$$

be the set of unit vectors that are closer to $\mathbf{g}_i$ than any other $\mathbf{g}_j \in \mathcal{G}$. Since $\cup_i \mathcal{D}_i = \mathbb{S}^2$, it is enough to show that

$$\min_i \min_{\mathbf{v} \in \mathcal{D}_i} \mathbf{g}_i^\mathsf{T} \mathbf{v} = \sqrt{\frac{1}{2}}.$$

As we now show, the regions $\mathcal{D}_1, \ldots, \mathcal{D}_{12}$ are congruent to each other. Let $\mathcal{H}$ be the symmetry group of the tetrahedron, i.e., the set of all orthogonal transformations on $\mathbb{R}^3$ that map the tetrahedron onto itself. It is known that the group $\mathcal{H}$ is isomorphic to the symmetric group $\mathcal{S}_4$ of degree 4, and every element of $\mathcal{H}$ is uniquely identified by its action on the set of vertices, which is isomorphic to the action of the corresponding element in $\mathcal{S}_4$ on the set $\{1, 2, 3, 4\}$ (see [23]). Since for any two given pairs (m_1, ℓ_1) and (m_2, ℓ_2), with $m_1 \neq \ell_1$ and $m_2 \neq \ell_2$, there exists a permutation on $\{1, 2, 3, 4\}$ that maps m_1 to m_2 and ℓ_1 to ℓ_2, we see that there exists an orthogonal transformation $\mathbf{M} \in \mathcal{H}$ such that

$$\mathbf{r}_{m_2} = \mathbf{M}\mathbf{r}_{m_1} \text{ and } \mathbf{r}_{\ell_2} = \mathbf{M}\mathbf{r}_{\ell_1}.$$

This can be extended to a group action on $\mathcal{G}$ as

$$\begin{aligned} \mathbf{M}\mathbf{g}_{m_1,\ell_1} &= \mathbf{M}\left(\frac{\mathbf{r}_{m_1} - \mathbf{r}_{\ell_1}}{\|\mathbf{r}_{m_1} - \mathbf{r}_{\ell_1}\|}\right) = \sqrt{\frac{3}{8}} \mathbf{M}\left(\mathbf{r}_{m_1} - \mathbf{r}_{\ell_1}\right) \\ &= \sqrt{\frac{3}{8}} \left(\mathbf{r}_{m_2} - \mathbf{r}_{\ell_2}\right) = \mathbf{g}_{m_2,\ell_2}. \end{aligned}$$

Thus, we see that the group $\mathcal{H}$ acts transitively on $\mathcal{G}$, i.e.,

$$\mathcal{G} = \{\mathbf{M}\mathbf{g}_i \,|\, \mathbf{M} \in \mathcal{H}\} \text{ for every } i = 1, \ldots, 12.$$

This makes $\mathcal{G}$ a group code, and consequently, the regions $\mathcal{D}_1, \ldots, \mathcal{D}_{12}$ are congruent to each other [22], i.e., for every $1 \leq i < j \leq 12$, there exists an orthogonal transformation $\mathbf{M} \in \mathcal{H}$ such that

$$\mathcal{D}_j = \mathbf{M}\mathcal{D}_i = \{\mathbf{M}\mathbf{v} \,|\, \mathbf{v} \in \mathcal{D}_i\}.$$

Since orthogonal transformations conserve inner products and since $\mathbf{g}_i \in \mathcal{D}_i$ for all i, we have

$$\min_{\mathbf{v} \in \mathcal{D}_i} \mathbf{g}_i^\mathsf{T} \mathbf{v} = \min_{\mathbf{v} \in \mathcal{D}_j} \mathbf{g}_j^\mathsf{T} \mathbf{v} \text{ for any } i \neq j.$$

Thus, to complete the proof, it is enough to show that

$$\min_{\mathbf{v} \in \mathcal{D}_1} \mathbf{g}_1^\mathsf{T} \mathbf{v} = \sqrt{\frac{1}{2}}.$$

We now restrict ourselves to one particular region $\mathcal{D}_1$ and find the smallest value of $\mathbf{g}_1^\mathsf{T} \mathbf{v}$. Note that when $\mathbf{v} \in \mathbb{S}^2$, the inner product of $\mathbf{v}$ with $\mathbf{g}_i$ decreases with increasing distance $\|\mathbf{v} - \mathbf{g}_i\|$. Thus, from (26), $\mathcal{D}_1$ is the intersection of $\mathbb{S}^2$ with the set of all points in $\mathbb{R}^3$ that are closer to $\mathbf{g}_1$ than any other $\mathbf{g}_i \in \mathcal{G}$. The region $\mathcal{D}_1$ is called a *fundamental region* of the group code $\mathcal{G}$ and is bounded by 2-D planes passing through the origin [22]. The half-spaces $\mathcal{P}_i$ that define this fundamental region are

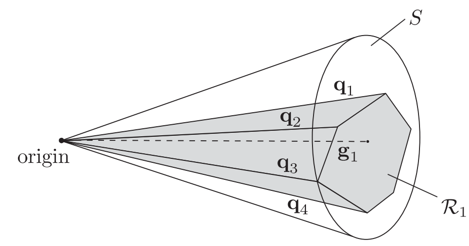

Fig. 6. Illustration of the cones S and $\mathcal{R}_1$ used in the proof of Proposition 1. The cone S is circular with axis $\mathbf{g}_1$ (dashed line). The cone $\mathcal{R}_1$ is bounded by hyperplanes, and its edges are along the vectors $\mathbf{q}_1, \ldots, \mathbf{q}_6$. The edge $\mathbf{q}_3$ is the farthest from the axis $\mathbf{g}_1$ and lies on the surface of S.

$$\begin{aligned} \mathcal{P}_i &= \left\{ \mathbf{x} \in \mathbb{R}^3 \,|\, \|\mathbf{x} - \mathbf{g}_1\| \leq \|\mathbf{x} - \mathbf{g}_i\| \right\} \\ &= \left\{ \mathbf{x} \in \mathbb{R}^3 \,|\, (\mathbf{g}_1 - \mathbf{g}_i)^\mathsf{T} \mathbf{x} \geq 0 \right\} \end{aligned}$$

and are related to $\mathcal{D}_1$ as

$$\mathcal{D}_1 = \mathbb{S}^2 \cap \mathcal{R}_1, \text{ where } \mathcal{R}_1 = \cap_{i=2}^{12} \mathcal{P}_i.$$

The group code $\mathcal{G}$ and the 11 half-spaces $\mathcal{P}_i$ can be explicitly calculated starting from the geometry of the tetrahedron, and it can be verified that $\mathcal{R}_1$, and hence $\mathcal{D}_1$, is bounded by exactly 6 planes arising from 6 of the 11 half-spaces $\mathcal{P}_i$. The region $\mathcal{R}_1$ is a convex cone [22] generated from the six edges running along the vectors $\mathbf{q}_1, \ldots, \mathbf{q}_6$ that are the intersections between the six hyperplanes, i.e., $\mathcal{R}_1$ is the infinite cone generated from the convex hull of the set $\{\mathbf{q}_1, \ldots, \mathbf{q}_6\}$. Fig. 6 shows an illustration of the geometry considered in this proof (the depiction of $\mathbf{q}_1, \ldots, \mathbf{q}_6$ is not exact). Since

$$\min_{\mathbf{v} \in \mathcal{D}_1} \mathbf{g}_1^\mathsf{T} \mathbf{v} = \min_{\mathbf{x} \in \mathcal{R}_1} \frac{\mathbf{g}_1^\mathsf{T} \mathbf{x}}{\|\mathbf{x}\|} \tag{27}$$

and since $\mathbf{g}_1^\mathsf{T} \mathbf{x} / \|\mathbf{x}\|$ is the cosine of the angle between $\mathbf{x}$ and $\mathbf{g}_1$, our problem is to find a vector in $\mathcal{R}_1$ that makes the largest angle with $\mathbf{g}_1$. The set of points that make a constant angle with $\mathbf{g}_1$ form the surface of an infinite circular cone with $\mathbf{g}_1$ as its axis. Thus, (27) is equivalent to finding the smallest circular cone S, with $\mathbf{g}_1$ as the axis, that contains the conical region $\mathcal{R}_1$. Since $\mathcal{R}_1$ is generated by $\mathbf{q}_1, \ldots, \mathbf{q}_6$, S is the smallest circular cone that contains the vectors $\mathbf{q}_1, \ldots, \mathbf{q}_6$, and has $\mathbf{g}_1$ as the axis. It follows that S contains on its surface the vector $\mathbf{q}_i$, from among $\mathbf{q}_1, \ldots, \mathbf{q}_6$, that makes the largest angle with $\mathbf{g}_1$. Thus,

$$\min_{\mathbf{v} \in \mathcal{D}_1} \mathbf{g}_1^\mathsf{T} \mathbf{v} = \min_{\mathbf{x} \in \mathcal{R}_1} \frac{\mathbf{g}_1^\mathsf{T} \mathbf{x}}{\|\mathbf{x}\|} = \min_{\mathbf{x} \in S} \frac{\mathbf{g}_1^\mathsf{T} \mathbf{x}}{\|\mathbf{x}\|}.$$

The numerical value $\min_{i \in \{1,\ldots,6\}} \mathbf{g}_1^\mathsf{T} \mathbf{q}_i \,/\, \|\mathbf{q}_i\| = 1/\sqrt{2}$ is obtained by a direct computation of the half-spaces $\mathcal{P}_1, \ldots, \mathcal{P}_{11}$, and the resulting vectors $\mathbf{q}_1, \ldots, \mathbf{q}_6$ arising from the tetrahedral geometry. ■

Proposition 2: If a tetrahedral array is used at the receiver and $\eta \geq 1$, then for every receive orientation $\mathbf{U}$, there exists a 2×2 submatrix $\mathbf{H}_{\text{sub}}$ of the channel matrix $\mathbf{H}$ such that

$$0 \leq \mu_{\text{sub}} \leq \cos\left(\frac{\pi}{2\sqrt{2}\eta}\right)$$

where μ_{sub} is the correlation between the two columns of $\mathbf{H}_{\mathrm{sub}}$.

Proof: From Proposition 1, there exist $m \neq \ell$ such that $\mathbf{g}_{m,\ell}^{\mathsf{T}}\mathbf{v} \geq \sqrt{1/2}$. Let $\mathbf{H}_{\mathrm{sub}}$ be the submatrix of $\mathbf{H}$ formed by the mth and ℓth rows. From (25) and the hypothesis that $\eta \geq 1$, we have $\mu_{\mathrm{sub}} = |\cos(\frac{\pi}{2\eta}\,\mathbf{g}_{m,\ell}^{\mathsf{T}}\mathbf{v})| \leq \cos(\frac{\pi}{2\eta}\sqrt{\frac{1}{2}})$. ■

The following upper bound on $\mu^*(\eta)$ follows immediately from Proposition 2.

Theorem 2: For a tetrahedral receive array and $\eta \geq 1$

$$\mu^*(\eta) \leq \frac{1}{2}\left(1 + \cos\left(\frac{\pi}{2\sqrt{2}\eta}\right)\right).$$

Proof: Let $\mathbf{H} = [h_{m,n}]$ be the 4×2 channel matrix. From Proposition 2, assume without loss of generality that the 2×2 submatrix formed from the first two rows has correlation $\mu_{\mathrm{sub}} \leq \cos(\pi/2\sqrt{2}\eta)$. Then

$$\begin{aligned}\mu &= \frac{1}{4}\left|h_{1,1}^{\dagger}h_{1,2} + h_{2,1}^{\dagger}h_{2,2} + h_{3,1}^{\dagger}h_{3,2} + h_{4,1}^{\dagger}h_{4,2}\right| \\ &\leq \frac{1}{4}\left|h_{1,1}^{\dagger}h_{1,2} + h_{2,1}^{\dagger}h_{2,2}\right| + \frac{1}{4}\left|h_{3,1}^{\dagger}h_{3,2} + h_{4,1}^{\dagger}h_{4,2}\right| \\ &= \frac{1}{2}\mu_{\mathrm{sub}} + \frac{1}{4}\left|h_{3,1}^{\dagger}h_{3,2} + h_{4,1}^{\dagger}h_{4,2}\right| \\ &\leq \frac{1}{2}\cos\left(\frac{\pi}{2\sqrt{2}\eta}\right) + \frac{2}{4}\end{aligned}$$

where the last inequality follows from Proposition 2 and the fact that all $h_{m,n}$ have unit magnitude. ■

The upper bound $(1 + \cos(\pi/2\sqrt{2}))/2$ on $\mu^*(\eta)$ is less than 1 for $\eta \geq 1$. Since $d(\mu, \Delta\mathbf{X})$ is a decreasing function of μ, we have $d(\mu^*(\eta), \Delta\mathbf{X}) > d(1, \Delta\mathbf{X})$. Hence, the geometry of the tetrahedral arrangement allows the error probability to decay faster than that of rank 1 LoS MIMO channels, and provides performance improvement over any planar arrangement $n_r = 4$ of antennas, irrespective of the code used at the transmitter. Note that this gain of the tetrahedral arrangement over planar arrays is not due to larger interantenna distances d_t and d_r.

From (21), we have $d(1, \Delta\mathbf{X}) \geq (\|\Delta\mathbf{x}_1\| - \|\Delta\mathbf{x}_2\|)^2$. Using $\mu^* < 1$, we obtain

$$d(\mu^*, \Delta\mathbf{X}) > d(1, \Delta\mathbf{X}) \geq (\|\Delta\mathbf{x}_1\| - \|\Delta\mathbf{x}_2\|)^2 \geq 0.$$

Hence, unlike the planar case, the error probability of a tetrahedral receiver is exponential in SNR for any code $\mathscr{C}$.

Example 5: Performance of spatial multiplexing with tetrahedral receive array. Consider the SM scheme signaled over $n_t = 2$ antennas using 4-QAM symbols. Let the transmit orientation $\beta = 0$ be fixed, the interterminal distance $R = 10$ m, $\lambda = 4.2$ mm, and $d_t = d_r = 0.145$ m. Then, $\eta = R\lambda/(2d_t d_r \cos\beta) = 1$, and from Theorem 2, $\mu^*(\eta) \leq 0.722$. An exhaustive numerical computation over all pairs of codewords yields $\min_{\Delta\mathbf{X}} d(0.722, \Delta\mathbf{X}) = 0.556$. Using (24), the pairwise error probability of SM for fixed transmit orientation and random receive orientation can be upper bounded as

$$\begin{aligned}\mathbb{E}(\mathsf{PEP}) \leq \mathsf{PEP}^* &\leq \frac{1}{2}\exp\left(-\mathsf{SNR}\,\mu^*(1)\right) \\ &\leq \frac{1}{2}\exp\left(-\mathsf{SNR} \times 0.556\right).\end{aligned}$$

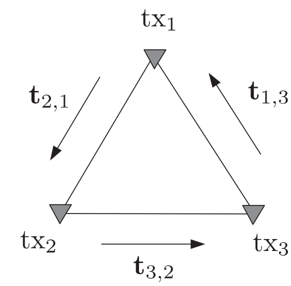

Fig. 7. Triangular arrangement of transmit antennas.

On the other hand, as shown in Example 4, for any planar receiver array, the error rate is not better than SNR^{-3}. ■

B. System Design for Arbitrary Array Orientations

In Section IV-A, we assumed that η was fixed, i.e., the transmit orientation β and interterminal distance R were fixed, and we studied the effect of an arbitrary rotation $\mathbf{U}$ of the receive array on μ and error probability. We now design a system that allows arbitrary transmit and receive array orientations and a range of values $R_{\min} \leq R \leq R_{\max}$. It is desirable that the LoS MIMO system guarantees a minimum channel quality, i.e., $\mu \leq \mu_{\max}$, for some $\mu_{\max} < 1$. Using (24), for such a system

$$\mathbb{E}(\mathsf{PEP}) \leq \mathsf{PEP}^* \leq \frac{1}{2}\exp\left(-\frac{n_r\,\mathsf{SNR}}{4}\,d(\mu_{\max}, \Delta\mathbf{X})\right).$$

Using union bound, the average codeword error rate and bit error rate of the system can be upper bounded by

$$\frac{|\mathscr{C}|}{2}\exp\left(-\frac{n_r\,\mathsf{SNR}}{4}\,\min_{\Delta\mathbf{X}} d(\mu_{\max}, \Delta\mathbf{X})\right).$$

Hence, the coding gain of an arbitrary coding scheme $\mathscr{C}$ over this LoS MIMO system is $\min_{\Delta\mathbf{X}} d(\mu_{\max}, \Delta\mathbf{X})$.

When the number of transmit antennas $n_t = 2$, by choosing $\beta = \pi/2$, we observe from (10) that the worst-case correlation $\mu_{\max} = 1$ irrespective of the array geometry used at the receiver. Hence, to have $\mu_{\max} < 1$, we need more than two antennas at the transmitter.

Suppose the transmitter uses an array of $n_t \geq 3$ antennas. Based on the transmit array orientation, one can choose two of the n_t antennas for signal transmission so that the angle β corresponding to the chosen pair of antennas is minimum. For example, let $n_t = 3$ antennas be placed at the vertices of an equilateral triangle with interantenna distance d_t, as shown in Fig. 7. Let $\mathbf{t}_{m,n}$ be the unit vector in $\mathbb{R}^3$ in the direction of the position of transmit antenna m with respect to the position of transmit antenna n. Note that the vectors $\mathbf{t}_{m,n}$ vary with changes in the transmit array orientation. If antennas m and n are used for transmission and if $\mathbf{u} \in \mathbb{R}^3$ is the unit vector along the direction OO' of transmission, then $\sin\beta = \mathbf{u}^{\mathsf{T}}\mathbf{t}_{m,n}$ (cf. Fig. 1, where tx_1 and tx_2 correspond to tx_m and tx_n, respectively). The six vectors in the set

$$\mathcal{T} = \{\mathbf{t}_{m,n}\,|\,m, n = 1, 2, 3,\ m \neq n\}$$

are arranged symmetrically in a 2-D plane at regular angular intervals of $\pi/3$. Let $\mathbf{u}_{\|}$ and $\mathbf{u}_{\perp}$ be the components of $\mathbf{u}$ parallel

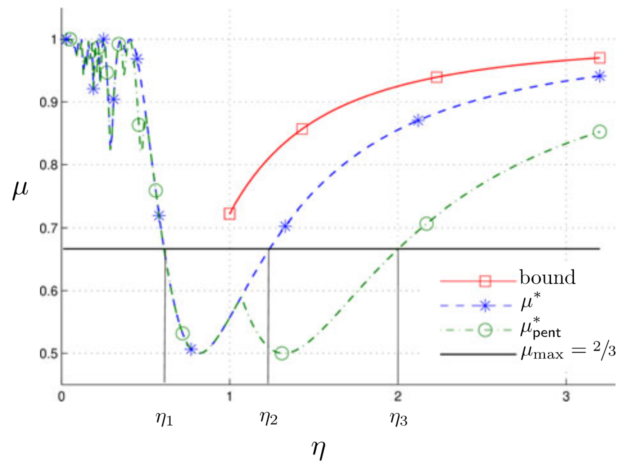

Fig. 8. Functions μ^*, μ^*_{pent}, upper bound on μ^*, and the line $\mu_{\max} = 2/3$.

and perpendicular to the plane of $\mathcal{T}$, respectively. Since the vectors in $\mathcal{T}$ divide the plane into regular conical regions of angular width $\pi/3$, there exists at least one vector $\mathbf{t}_{m,n} \in \mathcal{T}$ such that the angle between $\mathbf{t}_{m,n}$ and $\mathbf{u}_{\|}$ lies in the interval $[-\pi/6, +\pi/6]$, i.e.,

$$\frac{|\mathbf{u}_{\|}^{\mathsf{T}}\mathbf{t}_{m,n}|}{\|\mathbf{u}_{\|}\|} \leq \sin\left(\frac{\pi}{6}\right) = \frac{1}{2}.$$

We can, thus, upper bound $|\mathbf{u}^{\mathsf{T}}\mathbf{t}_{m,n}|^2$ as follows:

$$|\mathbf{u}^{\mathsf{T}}\mathbf{t}_{m,n}|^2 = |\mathbf{u}_{\perp}^{\mathsf{T}}\mathbf{t}_{m,n}|^2 + |\mathbf{u}_{\|}^{\mathsf{T}}\mathbf{t}_{m,n}|^2 \leq 0 + \|\mathbf{u}_{\|}\|^2\frac{1}{4} \leq \frac{1}{4}.$$

Thus, there exists a $\mathbf{t}_{m,n}$ such that

$$|\sin(\beta)| = |\mathbf{u}^{\mathsf{T}}\mathbf{t}_{m,n}| \leq \frac{1}{2}$$

i.e., $\beta \in [-\pi/6, \pi/6]$. Hence, if the transmit array is an equilateral triangle, by appropriately choosing two out of the three available antennas for signaling, one can ensure $|\beta| \leq \pi/6$.

The upper bound on $\mu^*(\eta)$ of Theorem 2 is not tight and is available only for $\eta \geq 1$. Since this bound cannot be used as a good estimate of $\mu^*(\eta)$ and the analytical computation of the exact expression (23) of $\mu^*(\eta)$ appears to be difficult, we use numerically computed values of $\mu^*(\eta)$ for system design. The function $\mu^*(\eta)$ and the upper bound of Theorem 2 are shown in Fig. 8. Using the exact function $\mu^*(\eta)$, the requirement on channel quality $\mu \leq \mu_{\max}$ can be translated into a criterion $\eta \in [\eta_{\min}, \eta_{\max}]$. From (22), for fixed d_t, d_r, λ, and $|\beta| \leq \beta_{\max}$, we have

$$\eta_{\min} = \frac{R_{\min}\lambda}{2d_t d_r} \text{ and } \eta_{\max} = \frac{R_{\max}\lambda}{2d_t d_r \cos\beta_{\max}}. \quad (28)$$

The range $[R_{\min}, R_{\max}]$ can thus be obtained from (28).

Example 6: Suppose we require $\mu_{\max} = 2/3$ with $\lambda = 4.2$ mm. Using a triangular transmit array, we have $\beta_{\max} = \pi/6$. From Fig. 8, the criterion $\mu^*(\eta) \leq 2/3$ is equivalent to $\eta_{\min} = \eta_1 = 0.62$, and $\eta_{\max} = \eta_2 = 1.22$. If each side of the triangular transmit array has length $d_t = 6$ cm, and the tetrahedral receive array has $d_r = 25$ cm, then from (28), we have $R_{\min} = 4.43$ m and $R_{\max} = 7.75$ m. ∎

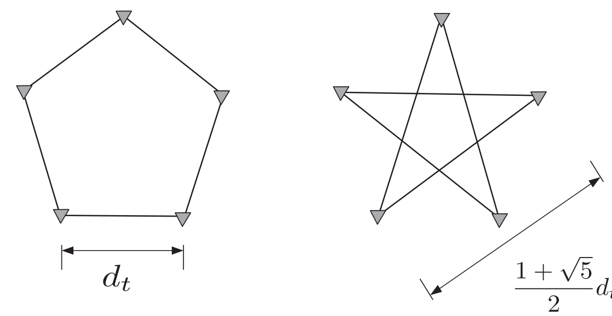

Fig. 9. Left: Any pair of neighboring antennas in a pentagonal array has an interantenna distance of d_t. Right: Any pair of non-neighboring antennas has distance $(1+\sqrt{5})d_t/2$.

The narrow range of $[R_{\min}, R_{\max}]$ in Example 6 can be attributed to the small value of $\eta_2 - \eta_1$ in Fig. 8. This can be improved by using a pentagonal transmit array as follows. As shown in Fig. 9, with a regular pentagon, the choice of the transmit antenna pair can be divided into the following two cases: 1) the two antennas are the neighboring vertices of the pentagon with interantenna distance equal to the length d_t of the edge of the regular pentagon, or 2) the antennas are non-neighboring with interantenna distance $(1+\sqrt{5})d_t/2$.

Irrespective of the class from which the antenna pair is chosen, it is straightforward to show that $|\beta| \leq \pi/10$ can be always guaranteed. While the value of η for the first case is given by (22), in the second case, it reduces by a factor of $(1+\sqrt{5})/2$ because of the larger interantenna distance. Thus, the maximum correlation with pentagonal transmit array is

$$\mu^*_{\mathsf{pent}}(\eta) = \min\left\{\mu^*(\eta), \mu^*\left(\frac{2\eta}{1+\sqrt{5}}\right)\right\}$$

where $\mu^*(\eta)$ is given in (23). From Fig. 8, the value of $\eta_{\max}$ improves from η_2 to η_3, thereby widening $[R_{\min}, R_{\max}]$.

Example 7: As in Example 6, let $\mu_{\max} = 2/3$, $\lambda = 4.2$ mm, $d_t = 6$ cm, and $d_r = 25$ cm. With a pentagonal transmit array, $\beta_{\max} = \pi/10$, and using the function μ^*_{pent}, we have $\eta_{\min} = \eta_1 = 0.62$, and $\eta_{\max} = \eta_3 = 2$. Using (28), $R_{\min} = 4.43$ m, and $R_{\max} = 12.7$ m. ∎

V. Simulation Results

We use the system parameters λ, d_t, d_r, $R_{\max}$, and $R_{\min}$ from Example 7. We assume that the transmit and receive arrays undergo independent uniformly random 3-D rotations about their centroids, and the distance R between the terminals is uniformly distributed in $[R_{\min}, R_{\max}]$. In all the simulations, the channel matrix $\mathbf{H}$ was synthesized using (1) and the exact distances $\{r_{m,n}\}$ between the transmit and the receive antennas. We consider the following three coding schemes with the transmission rate of 4 bits per channel use:

1) the Golden code [19] using 4-QAM alphabet,
2) SM [15]–[17] with 4-QAM, and
3) uncoded 16-QAM transmitted using only one transmit antenna [single-input multiple-output (SIMO)].

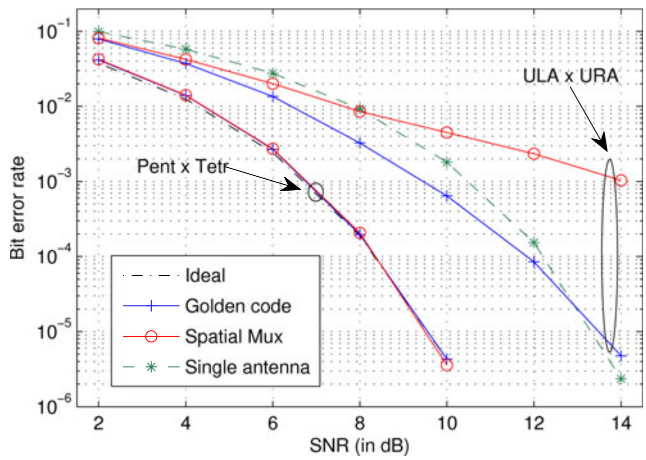

Fig. 10. Comparison of Pent $\times$ Tetr with ULA $\times$ URA.

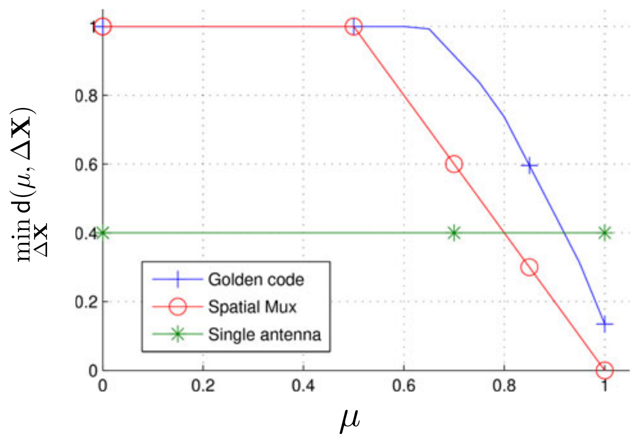

Fig. 11. Coding gain for bit rate of 4 bits per channel use.

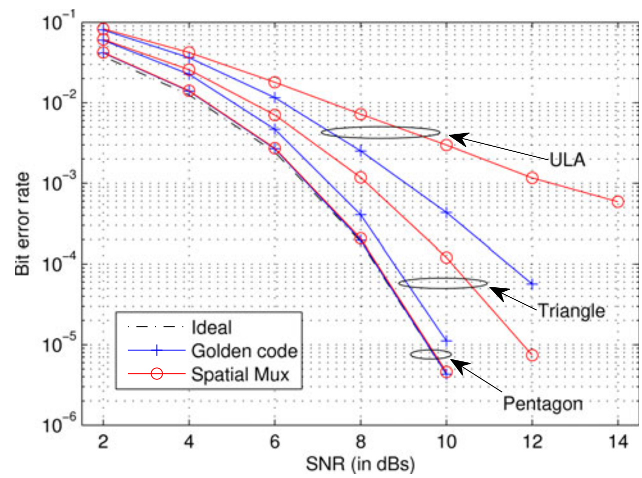

Fig. 12. Performance of different tx arrays with tetrahedral rx array.

Gray mapping is used at the transmitter to map information bits to constellation points, and unless otherwise stated, ML decoding is performed at the receiver. While we used pairwise error probability for the performance analysis in Sections II, III, and IV, we simulate the bit error rate to compare the average error performance.

A. *Error Performance With $n_r = 4$*

Fig. 10 shows the performance of the three schemes with two different antenna geometries: 1) ULA at the transmitter with $n_t = 2$, and uniform rectangular array (URA) at receiver[2] with $n_r = 4$, and 2) selecting two antennas from a pentagonal array at the transmitter, and using a tetrahedral array at the receiver. The values of d_t, d_r are ideal for the ULA $\times$ URA configuration [5] at the distance $R = 2d_t d_r/\lambda = 7.14$ m, which is near the midpoint of the interval $[R_{\min}, R_{\max}]$. The performance of the single-antenna transmission scheme is independent of the receive antenna geometry since, from (1), all the channel gains of the SIMO channel have unit magnitude. Also, Fig. 10 shows the performance of the ideal channel with $\mu = 0$, i.e., $\mathbf{R} = \sqrt{n_r}\,\mathbf{I}_2$, which is a pair of parallel additive white Gaussian noise channels, each carrying a 4-QAM symbol. From Fig. 10, we see that, with ULA $\times$ URA, the performance of both SM and the Golden code is worse than SIMO at high SNR. Furthermore, since $\min_{\Delta\mathbf{X}} d(1, \Delta\mathbf{X}) = 0$ for SM, the error probability decays slowly with SNR, confirming our theoretical results. With the proposed pentagon$\times$tetrahedron geometry, both codes show improved performance, close to that of the ideal channel.

The above error performance is succinctly captured by the coding gain $\min_{\Delta\mathbf{X}} d(\mu, \Delta\mathbf{X})$ shown in Fig. 11 as a function of μ. From Example 7, $\mu \leq 2/3$ for the new antenna geometry. From Fig. 11, we see that the coding gains of SM and the Golden code are both equal to 1 for all $\mu \leq 1/2$ and are larger than the SIMO coding gain for $\mu \leq 2/3$, which explains their superiority to SIMO. On the other hand, the coding gain for linear and rectangular arrays is $\min_{\Delta\mathbf{X}} d(1, \Delta\mathbf{X})$. For $\mu = 1$, from Fig. 11, we observe that SIMO has the largest coding gain followed by the Golden code and then SM. The error performances in Fig. 10 show this same trend for the rectangular array at high SNR.

Fig. 12 compares the performance of different transmit array geometries when a tetrahedral array is used at the receiver. The $n_t = 2$ case (ULA) performs poorly since $\mu_{\max} = 1$. While the triangular array with the Golden code achieves most of the available gain, the pentagonal array has near ideal performance.

B. *Error Performance With Large Number of Receive Antennas*

The LoS MIMO system analyzed in Section IV employs the tetrahedral receive array—a 3-D antenna array for $n_r = 4$ antennas—to enable smaller error rates than planar arrays. The geometry of the receive array is relevant even if the number of receiving antennas n_r is large. Theorem 1 and Example 4 show that the probability of error of the SM scheme is lower bounded up to a constant factor by SNR^{-3} for any value of n_r, if a planar receive array is used. On the contrary, from Example 5, the SM scheme can achieve exponential rate of decay of error probability, if $n_r = 4$ antennas are placed at the vertices of a

[2]The performance of uniform linear array at receiver is worse than that of URA, and hence has been omitted.

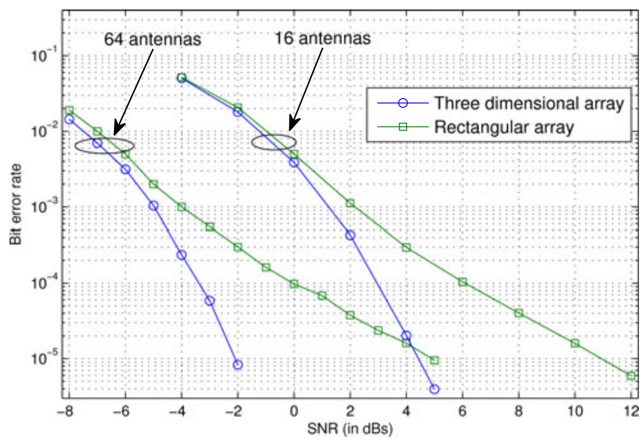

Fig. 13. Error probability of spatial multiplexing with triangular transmit array when the receive array is (i) three-dimensional, and (ii) rectangular. Results are shown for $n_r = 16$ and $n_r = 64$ antennas.

regular tetrahedron. It follows that for any $n_r \geq 4$, a careful 3-D arrangement of n_r antennas can ensure that the error rate is exponential in SNR. For instance, if the 3-D arrangement includes a subset of four antennas that form a tetrahedron, it immediately follows from Example 5 that a suboptimal decoder that bases its decision only on the signals received by these four antennas achieves exponential error rate. Hence, the optimal ML decoder that utilizes all the n_r receive antennas achieves an exponential error probability as well.

Fig. 13 compares the error performance of SM scheme under planar and 3-D receive antenna arrays when $n_r = 16, 64$. A triangular array is used at the transmitter, 4-QAM is chosen as the modulation scheme, and ML decoding is performed at the receiver. For both values of n_r, we consider a URA (rectangular arrangement of receive antennas) for the planar arrangement of antennas. The 3-D array is chosen as a set of n_r points on the surface of a sphere so that the minimum distance between the points is large. A table of such arrangements of points, which are known as *spherical codes*, is available online [24]. For fairness, the diameter of the sphere is set equal to the width of the rectangular array. The coordinates of the n_r points on the sphere were obtained from [24]. As with previous simulations, we set the values of d_t, λ, $R_{\max}$, and $R_{\min}$ as in Example 7. The interantenna distance d_r of the URA is chosen to be 12.5 cm when $n_r = 16$ and to be 6.25 cm when $n_r = 64$. This is the optimal interantenna distance for the URA when the transmit and receive arrays are oriented broadside to each other, and the interterminal distance $R = 7.14$ m [5].

It is evident from Fig. 13 that array geometry is an important design parameter even when n_r is large. The error rates of rectangular arrays shown in Fig. 13 decay as SNR^{-2} at high SNR. The gain due to the 3-D array is about 7 dB at an error rate of 10^{-5} for both $n_r = 16$ and 64.

VI. Conclusion

We studied the error performance of arbitrary coding schemes in $2 \times n_r$ LoS MIMO channels where the communicating terminals have random orientations. We analyzed the effects of some receive array geometries on error probability and showed that, unlike linear, circular, and rectangular arrays, the error rate with a tetrahedral array decays faster than that of a rank 1 channel. Using tetrahedral and polygonal arrays, we designed a LoS MIMO system that provides a good error performance for all transmit and receive orientations. By modeling the $\mathbf{R}$ matrix, we derived error probability bounds for the case when the number of transmit antennas used for signaling is 2. Analysis of the performance when more than two transmit antennas are used is yet to be addressed.

Acknowledgment

The authors would like to thank the anonymous reviewers and the editor for their constructive comments that have improved the content and the presentation of this paper.

References

[1] T. Rappaport *et al.*, "Millimeter wave mobile communications for 5G cellular: It will work!" *IEEE Access*, vol. 1, pp. 335–349, 2013.
[2] E. Torkildson, U. Madhow, and M. Rodwell, "Indoor millimeter wave MIMO: Feasibility and performance," *IEEE Trans. Wireless Commun.*, vol. 10, no. 12, pp. 4150–4160, Dec. 2011.
[3] F. Bohagen, P. Orten, and G. Oien, "Construction and capacity analysis of high-rank line-of-sight MIMO channels," in *Proc. 2005 IEEE Wireless Commun. Netw. Conf.*, vol. 1, Mar. 2005, pp. 432–437.
[4] F. Bohagen, P. Orten, and G. Oien, "Design of optimal high-rank line-of-sight MIMO channels," *IEEE Trans. Wireless Commun.*, vol. 6, no. 4, pp. 1420–1425, Apr. 2007.
[5] F. Bohagen, P. Orten, and G. Oien, "Optimal design of uniform rectangular antenna arrays for strong line-of-sight MIMO channels," *EURASIP J. Wireless Commun. Netw.*, vol. 2007, no. 2, Jan. 2007, Art. no. 45084.
[6] I. Sarris and A. Nix, "Design and performance assessment of high-capacity MIMO architectures in the presence of a line-of-sight component," *IEEE Trans. Veh. Technol.*, vol. 56, no. 4, pp. 2194–2202, Jul. 2007.
[7] T. Cella and P. Orten, "Improving coverage in mm-wave system by optimized MIMO geometry," in *Proc. 2013 Int. Conf. Wireless Commun. Signal Process.*, Oct. 2013, pp. 1–6.
[8] P. Wang, Y. Li, X. Yuan, L. Song, and B. Vucetic, "Tens of gigabits wireless communications over E-band LoS MIMO channels with uniform linear antenna arrays," *IEEE Trans. Wireless Commun.*, vol. 13, no. 7, pp. 3791–3805, Jul. 2014.
[9] P. Wang, Y. Li, X. Yuan, L. Song, and B. Vucetic, "Millimeter wave wireless transmissions at E-band channels with uniform linear antenna arrays: Beyond the Rayleigh distance," in *Proc. IEEE Int. Conf. Commun.*, Jun. 2014, pp. 5455–5460.
[10] C. Hofmann, A. Knopp, and B. Lankl, "Indoor LoS MIMO channel measurements with a focus on antenna array design," in *Proc. IEEE Glob. Telecommun. Conf.*, Dec. 2010, pp. 1–5.
[11] B. N. Getu and J. B. Andersen, "The MIMO cube—A compact MIMO antenna," *IEEE Trans. Wireless Commun.*, vol. 4, no. 3, pp. 1136–1141, May 2005.
[12] C. Y. Chiu, J. B. Yan, and R. D. Murch, "24-port and 36-port antenna cubes suitable for MIMO wireless communications," *IEEE Trans. Antennas Propag.*, vol. 56, no. 4, pp. 1170–1176, Apr. 2008.
[13] D. T. Le, M. Shinozawa, and Y. Karasawa, "Novel compact antennas for MIMO wireless communication systems," in *Proc. 2010 Int. Conf. Adv. Technol. Commun.*, Oct. 2010, pp. 341–345.
[14] D. Park and D. H. Cho, "Analysis of pattern gain of compact directional 16-port antenna," *IEEE Antennas Wireless Propag. Lett.*, vol. 14, pp. 902–905, 2015.
[15] G. J. Foschini, "Layered space-time architecture for wireless communication in a fading environment when using multi-element antennas," *Bell Labs Tech. J.*, vol. 1, no. 2, pp. 41–59, 1996.
[16] P. Wolniansky, G. Foschini, G. Golden, and R. Valenzuela, "V-BLAST: An architecture for realizing very high data rates over the rich-scattering wireless channel," in *Proc. URSI Int. Symp. Signals, Syst., Electron.*, Sep. 1998, pp. 295–300.

[17] E. Telatar, "Capacity of multi-antenna Gaussian channels," *Eur. Trans. Telecommun.*, vol. 10, no. 6, pp. 585–595, 1999.
[18] V. Tarokh, N. Seshadri, and A. Calderbank, "Space-time codes for high data rate wireless communication: Performance criterion and code construction," *IEEE Trans. Inf. Theory*, vol. 44, no. 2, pp. 744–765, Mar. 1998.
[19] J. C. Belfiore, G. Rekaya, and E. Viterbo, "The Golden code: A 2×2 full-rate space-time code with nonvanishing determinants," *IEEE Trans. Inf. Theory*, vol. 51, no. 4, pp. 1432–1436, Apr. 2005.
[20] M. Abramowitz and I. A. Stegun, *Handbook of Mathematical Functions With Formulas, Graphs, and Mathematical Tables* (National Bureau of Standards Applied Mathematics Series), vol. 55. Washington, DC, USA: U.S. Government Printing Office, 1964.
[21] A. Baricz, "Mills' ratio: Monotonicity patterns and functional inequalities," *J. Math. Anal. Appl.*, vol. 340, no. 2, pp. 1362–1370, 2008.
[22] D. Slepian, "Group codes for the Gaussian channel," *Bell Syst. Tech. J.*, vol. 47, no. 4, pp. 575–602, 1968.
[23] W. Miller, *Symmetry Groups and Their Applications*, vol. 50. New York, NY, USA: Academic, 1973.
[24] N. J. A. Sloane (with the collaboration of R. H. Hardin, W. D. Smith, and others), *Tables of Spherical Codes*. [Online]. Available: http://www.neilsloane.com/packings/

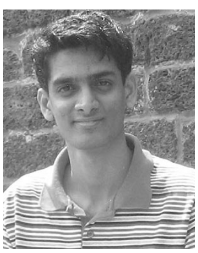

Lakshmi Natarajan received the B.E. degree in electronics and communication from the College of Engineering, Guindy, India, in 2008, and the Ph.D. degree in electrical communication engineering from the Indian Institute of Science, Bangalore, India, in 2013.

From 2014 to 2016, he held a Postdoctoral position in the Department of Electrical and Computer Systems Engineering, Monash University, Melbourne, VIC, Australia. He is currently an Assistant Professor in the Department of Electrical Engineering, Indian Institute of Technology, Hyderabad, India. His primary research interests include modulation, coding, and signal processing for multiterminal and multi-antenna communication systems.

Dr. Natarajan received the Seshagiri-Kaikini Medal 2013–14 for the best Ph.D. thesis, Department of Electrical Communication Engineering, Indian Institute of Science, Bangalore. He was recognized as an Exemplary Reviewer by the editorial board of the IEEE WIRELESS COMMUNICATIONS LETTERS in 2013 and 2015. He served as the Local Arrangements Co-Chair of the 2016 Australian Communications Theory Workshop, Melbourne, and the 2016 Australian Information Theory School, Melbourne.

Yi Hong (M'00–SM'10) received the Ph.D. degree in electrical engineering and telecommunications from the University of New South Wales (UNSW), Sydney, Australia, in 2004.

She is currently a Senior Lecturer in the Department of Electrical and Computer Systems Engineering, Monash University, Clayton, Australia. Her research interests include communication theory, coding, and information theory with applications to telecommunication engineering.

Dr. Hong received an International Postgraduate Research Scholarship from the Commonwealth of Australia and a Supplementary Engineering Award from the School of Electrical Engineering and Telecommunications, UNSW, during the Ph.D. degree candidacy. She received the NICTA-ACoRN Early Career Researcher Award for a paper presented at the Australian Communication Theory Workshop, Adelaide, 2007. She is an Associate Editor of the IEEE WIRELESS COMMUNICATIONS LETTERS and the *European Transactions on Telecommunications*. She was the General Co-Chair of the 2014 IEEE Information Theory Workshop, Hobart, Tasmania; and the Technical Program Committee Chair of the 2011 Australian Communications Theory Workshop, Melbourne, Australia. She was the Publicity Chair at the 2015 International Conference on Telecommunications, Sydney, and the 2009 IEEE Information Theory Workshop, Sicily, Italy.

Emanuele Viterbo (M'95–SM'04–F'11) was born in Torino, Italy, in 1966. He received the degree (Laurea) and the Ph.D. degree both in electrical engineering from the Politecnico di Torino, Torino, Italy, in 1989 and 1995, respectively.

From 1990 to 1992, he was in the European Patent Office, The Hague, The Netherlands, as a Patent Examiner in the field of dynamic recording and error-control coding. In 1993, he was a Visiting Researcher in the Communications Department of DLR, Oberpfaffenhofen, Germany. In 1994 and 1995, he was visiting the Ecole Nationale Superieure des Telecommunications, Paris, France. From 1995 to 1997, he held a Postdoctoral position in the Dipartimento di Elettronica of the Politecnico di Torino in Communications Techniques over Fading Channels. In 1998, he was a Visiting Researcher in the Information Sciences Research Center, AT&T Research, Florham Park, NJ, USA. In 2003, he was a Visiting Researcher in the Maths Department, Ecole Polytechnique Federale de Lausanne, Lausanne, Switzerland. In 2004, he was a Visiting Researcher in the Telecommunications Department, University of Campinas, Campinas, Brazil. In 2005, he was a Visiting Researcher in the Institute for Telecommunications Research, University of South Australia, Adelaide, Australia. He became an Associate Professor in the Politecnico di Torino, Dipartimento di Elettronica, in 2005, and a Full Professor in Department of Electronics, Computer Science and Systems, Università della Calabria, Arcavacata, Italy, in 2006. Since 2010, he has been a Full Professor in the Department of Electrical and Computer Systems Engineering and the Associate Dean Graduate Research of the Faculty of Engineering, Monash University, Melbourne, Australia, His main research interests include lattice codes for the Gaussian and fading channels, algebraic coding theory, algebraic space-time coding, digital terrestrial television broadcasting, and digital magnetic recording.

Dr. Viterbo received a NATO Advanced Fellowship in 1997 from the Italian National Research Council. He was an Associate Editor of the IEEE TRANSACTIONS ON INFORMATION THEORY, the *European Transactions on Telecommunications*, and the *Journal of Communications and Networks*. He is currently an Editor of the *Foundations and Trends in Communications and Information Theory*.